



ANALYTICAL STUDY OF THE CIRCULATION OF JAMES BAY

DFO - Library / MPO - Bibliothèque

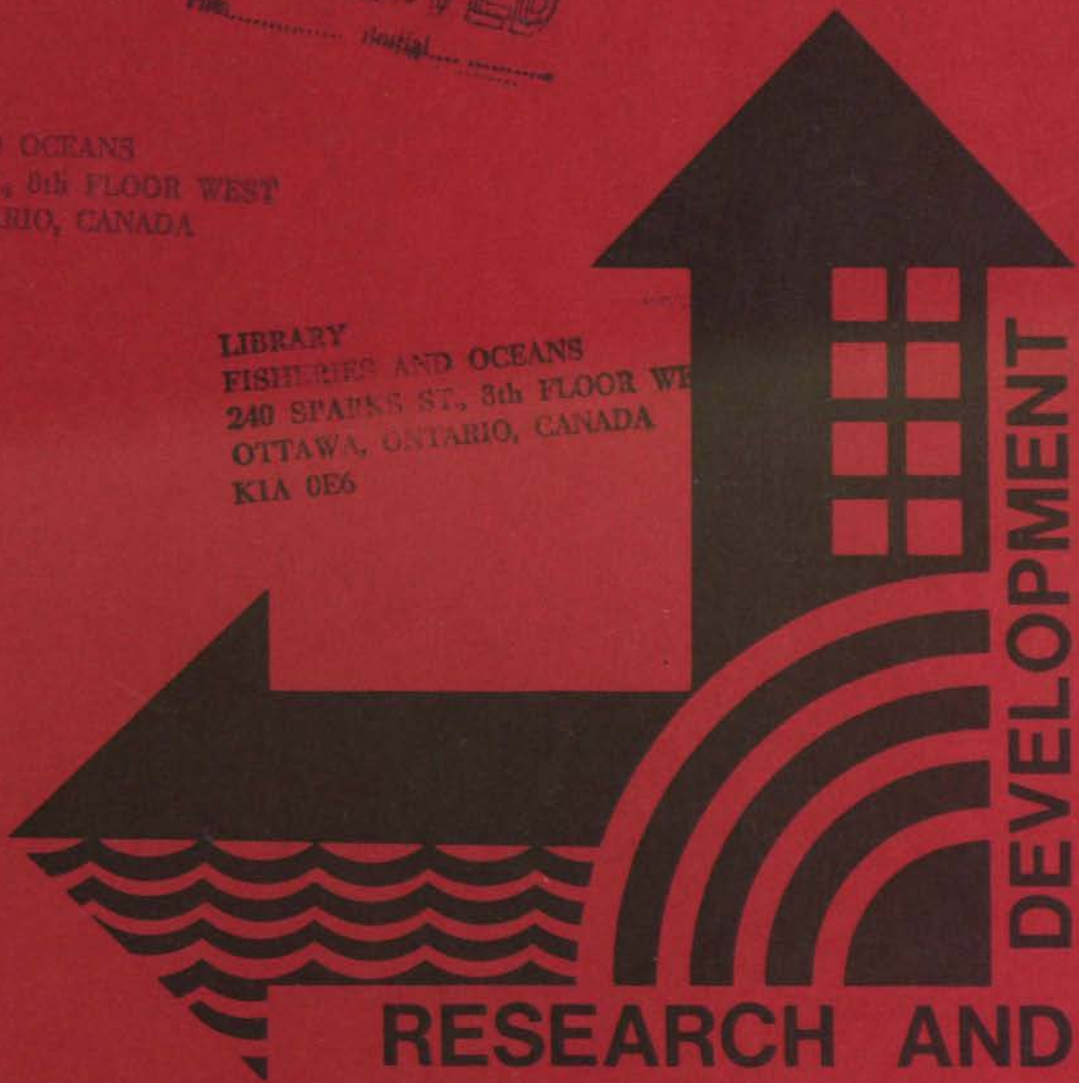
12045398

OCEANOGRAPHIC RESEARCH
RECEIVED
RECEIVED
File..... Initial.....

S.J. PRINSEBERG

LIBRARY
FISHERIES AND OCEANS
240 SPARKS ST., 8th FLOOR WEST
OTTAWA, ONTARIO, CANADA
K1A 0E6

LIBRARY
FISHERIES AND OCEANS
240 SPARKS ST., 8th FLOOR WE
OTTAWA, ONTARIO, CANADA
K1A 0E6



DEVELOPMENT
RESEARCH AND

OCEAN AND AQUATIC SCIENCES
CENTRAL REGION

CANADA CENTRE FOR INLAND WATERS
BURLINGTON, ONTARIO

GB
651
M361
no. 6

ANALYTICAL STUDY
OF THE
CIRCULATION OF JAMES BAY

by

S.J. Prinsenber

This is an internal technical report which has received only limited circulation. On citing this report, the reference should be followed by the words "UNPUBLISHED MANUSCRIPT."

October, 1978

P.O. Box 5050
Burlington, Ontario
L7R 4A6

ABSTRACT

Factors determining the circulation of James Bay are studied using oceanographic station and time-series current meter data. Water from Hudson Bay enters into James Bay over the total bottom layer as well as in the surface layer for the western half of the entrance. The low salinity surface water entering the bay is diluted even further by the large runoff of the James Bay rivers. The surface outflow at the James Bay entrance is restricted to a depth of 30 metres and reaches speeds of up to 20 cm sec^{-1} .

For cross-sectional averaged salinity and velocity profiles, the analytical model reveals that the circulation in James Bay is a combination of the gravitational and wind-driven circulations. Northerly winds, with speeds greater than 20 knots, reverse the direction of the surface current and can set up a three-layered velocity profile with inflows at the top and bottom and an outflow at mid depth. The gravitational circulation is caused by the horizontal density gradient which, in turn, is enhanced by the runoff dilution. Changes in runoff will thus show up in circulation changes via the gravitational circulation. The gravitational circulation becomes even more important during the winter, as then it is the only one that causes circulation since the ice friction, considered as a negative wind stress, opposes the circulation.

Circulation at the entrance of James Bay is classified as a stratified fjord which means that the upstream salt flux is mainly achieved by advection. This was also found by inspection of the terms in the conservation of salt equation. The circulation properties for the transect off Fort George become more comparable to that of a strongly-stratified, mixed estuary during the summer and to that of a weakly-stratified, mixed estuary during the winter. Upstream salt flux is achieved by both advection and diffusion, with diffusion becoming increasingly important as the stratification and current values decrease during the fall and winter.

The mean salinity and velocity profiles obtained by the analytical model compare well with those obtained from observed data. The extreme low salinity and high current values found in the surface outflow along the

Quebec coast are not predicted, as only cross-sectional mean values can be obtained. When the hydroelectric development along the La Grande River is completed, the model predicts that, for the future winter runoff rates, the surface current along the Quebec coast will double and that its dilution effect could be felt at the Belcher Islands within 50 days of the formation of a solid ice cover.

ACKNOWLEDGMENTS

The author would like to thank Drs. T.S. Murty and M.I. El-Sabh for reading and suggesting changes to the manuscript and Messrs. N.G. Freeman and S. Peck for their numerous discussions of the work as well as for reading the first draft.

Mrs. C. Kennedy and Mr. B. Thorson overviewed respectively the editorial and cartographic work of the report.

TABLE OF CONTENTS

	<u>Page</u>
Abstract	i
Acknowledgments	iii
Table of Contents	v
List of Figures	vi
List of Tables	vii
CHAPTER 1	
1.0 Introduction	1
CHAPTER 2	
2.0 Oceanographic Parameters	3
2.1 Topography	3
2.2 Oceanographic Parameter Distributions of Hudson Bay	6
2.3 Oceanographic Parameter Distributions of James Bay	11
CHAPTER 3	
3.0 Theoretical Determination of the Circulation Contributions	17
3.1 Conservation of Salt Equations	17
3.2 Analytical Models	21
3.3 Estuarine Classification	27
CHAPTER 4	
4.0 Analytical Results	31
4.1 Summer Analytical Results	31
4.2 Coriolis Effect	38
4.3 Winter Analytical Results	40
4.4 Possible Salinity and Current Changes Due to the La Grande River Hydroelectric Development	42
CHAPTER 5	
5.0 Conclusion	45
References	47
Appendix	49

LIST OF FIGURES

<u>Figure</u>		<u>Page</u>
1	Bathymetry of Hudson Bay	4
2	Bathymetry of James Bay	5
3	Surface Salinity Distribution of Hudson Bay for the Summer of 1975	7
4	Surface Temperature Distribution of Hudson Bay for the Summer of 1975	8
5	Surface Salinity and Temperature Distribution of James Bay for September 1972	12
6	Surface Salinity Distributions of James Bay for the Winters of 1975 and 1976	13
7	Cross-Sectional (West-East) Salinity, Temperature, and Density Distributions at the Entrance of James Bay	14
8	Cross-Sectional (South-North) Salinity, Temperature, and Density Distributions North of the Entrance of James Bay	15
9	Transect Areas of James Bay used in the Freshwater Input Distribution	19
10	Monthly Freshwater Input and Transect Salinity Values for James Bay	19
11	Estuary Classification of James Bay Transects 1 and 3	28
12	Analytical and Observational Results for different Summer Wind Stress (T/4) Conditions (Positive velocity value means a flow out of the bay, northward).	33
13	Locations of Current Meters Relative to Salinity Distribution as observed during Retrieval of Meters (September 17, 1975)	35
14	Tidal (M_2) and Mean Velocities for Four Current Meters located at 10-Metre Depth at Arrays 1A and 4A, 60-Metre Depth at Array 1A and 70-Metre Depth at Array 4A	37
15	Analytical and Observational Results for the Present and Future Predicted Winter Conditions (Positive velocity value means a flow out of the bay, northward).	41

LIST OF TABLES

<u>Table</u>		<u>Page</u>
A-1	Cross-Sectional Mean Salinity - Depth Profiles for Transect 1	51
A-2	Cross-Sectional Mean Salinity - Depth Profiles for Transect 3	51
A-3	Estuarine Classification Parameters for Transects 1 and 3 of James Bay	52
A-4	Total Monthly Freshwater Input for each of the James Bay Areas.	53
A-5	Monthly Freshwater Velocity Values through each James Bay Transect	54
A-6	Mean Drift Velocity for the Summer of 1975 at the Entrance of James Bay	55

CHAPTER 1

1.0 Introduction

The hydroelectric development on the La Grande River, scheduled for completion by 1986, will modify the yearly cycle of the freshwater input of the La Grande and Eastmain estuaries. For the total James Bay area, the freshwater input from river runoff will be changed temporarily as well as spatially. The constant year-round planned runoff rate for the La Grande River, entering James Bay at Fort George, will be just below the present averaged spring maximum runoff rate with the additional water coming from the headwaters of the Eastmain and Koksoak Rivers. In order to speculate on the probable modifications on the circulation and distribution of oceanographic parameters, the transport of oceanographic parameters between James Bay and Hudson Bay and the present freshwater budget of James Bay have to be understood. Oceanographic "station" data, consisting of vertical depth distribution profiles of salinity and temperature, are used to study the horizontal distribution of the parameters in James Bay and in the boundary area between Hudson Bay and James Bay. "Time-series" data, obtained from in-situ moored instruments measuring current speed and direction, temperature, and conductivity, are used to study the boundary transport conditions between James Bay and Hudson Bay. However, these boundary conditions can only be obtained at certain times of the year when a survey from an oceanographic vessel (summer) or from a helicopter (winter) can operate in the region. Large time gaps between winter and summer baseline data thus exist, and time-series data at the entrance of the bay have only been obtained during the summer months.

The first studies of the James Bay area were usually done as part of the studies for the combined Hudson/James Bay region. An oceanographic parameter distribution for the combined region was presented by Barber (1967) using all the available oceanographic data up to 1962, while a monthly-averaged heat budget of the combined region was carried out by Danielson (1969). Special attention was given to James Bay in 1972 when the distribution of oceanographic parameters (Barber), the tides (Godin), and the circulation (Murty) of James Bay were investigated. All pointed out the

need for more oceanographic and bathymetric data in order to understand the physical processes occurring in James Bay that may be altered by the planned hydroelectric development on the James Bay rivers.

The additional summer oceanographic data obtained between 1972 and 1974 was used in the physical oceanographic study of James Bay by El-Sabh and Koutitonsky (1977). It was the first study that used the oceanographic "station" data and attempted to distinguish the individual contributors and surface boundary conditions that determine the summer transports between Hudson Bay and James Bay. Multidisciplinary winter surveys of 1975 (McCarthy and Boyd) and 1976 (Wright) collected baywide oceanographic, bathymetric, and gravity data during the ice-covered season of James Bay. This oceanographic data, in addition to the available summer data collected in the La Grande River estuary, was presented at the James Bay Environmental Symposium (Peck, 1976a). This manuscript will concentrate on the contributions to the transport between Hudson Bay and James Bay using oceanographic "station" data, in-situ current meter data, river runoff data, and meteorological data. Both winter and summer distributions of the salinity and circulation will be investigated for the present runoff rates and for the winter using predicted runoff rates. With a simple analytical model, the circulation is shown to consist of three contributions: the wind-driven circulation, the freshwater circulation dispensing the added freshwater volume, and the gravitational circulation caused by the density difference between the sea water at the entrance and the diluted water within James Bay. The latter, gravitational circulation, is also referred to in texts as the thermohaline circulation. The relative importance of the three contributors to the total circulation as well as of the horizontal diffusion and advection of the upstream salt flux is discussed.

CHAPTER 2

2.0 Oceanographic Parameters

Since James Bay is connected to Hudson Bay, it will be necessary to first discuss some of the known physical properties of the combined area. The topographic features and the general summer circulation pattern, as inferred from the horizontal oceanographic parameter distribution, will be presented for Hudson Bay so that the possible exchange properties between the two bays can be more easily understood.

2.1 Topography

The Hudson/James Bay area is part of a larger aquatic system that also includes Foxe Basin, Foxe Channel, and Hudson Strait. The combined system is connected to the Atlantic Ocean in the south via the Labrador Sea and to the Arctic Ocean in the north via the Fury and Hecla Straits and other straits surrounding the Canadian Arctic islands. Except for a minor sill between Coats and Mansel Islands, the waters of Hudson and James Bays are not restricted in their movement to and from the Atlantic Ocean. The sill depth of 197 metres will affect only a small portion of the bottom waters of Hudson Bay, since most of the area is less than 200 metres deep with only two areas reaching depths of 235 metres (Figure 1). The other two channels connecting Hudson Bay and Hudson Straits are between Southampton and Coats Islands and between the Ungava Peninsula (northern Quebec mainland) and Mansel Island. These two channels restrict water exchange between the bay and the strait below depths of 130 metres. A fourth smaller channel at the extension of Roes Welcome Sound can be ignored when the deep-water exchange between the bay and the strait are considered. The deep-water exchange below 130 metres occurs only in the middle channel, whereas shallow-water exchange can occur in all three channels. The topographic features of Hudson Bay are very gentle in character, with only the eastern shore and the Belcher Islands region showing some rugged sills and trenches. The average depth of the bay is about 125 metres and, when the Belcher Islands are ignored, the bay has a rectangular shape of 925 by 700 kilometres.

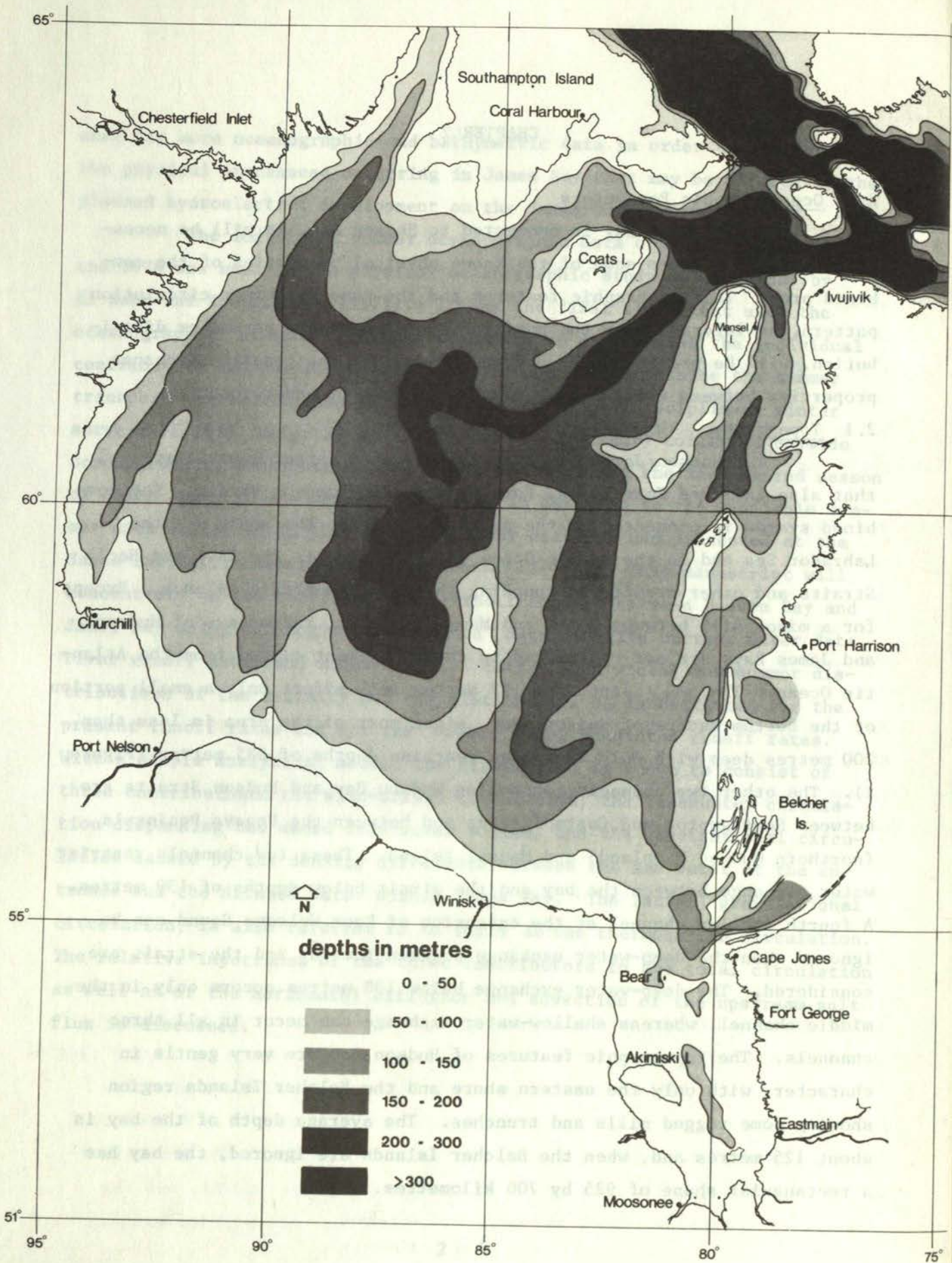


Figure 1: Bathymetry of Hudson Bay

A sill between Cape Henrietta Maria (northern Ontario) and the Belcher Islands has a maximum depth of 80 metres. It represents the largest depth at which uninterrupted horizontal deep-water exchange between Hudson Bay and James Bay can exist. The other sills in the northeast between the Belcher Islands and Ungava Peninsula all have shallow maximum depths. The sill, however, does not symbolize a major restriction to the deep-water exchange, since only a small portion of the James Bay area has a depth greater than 80 metres.

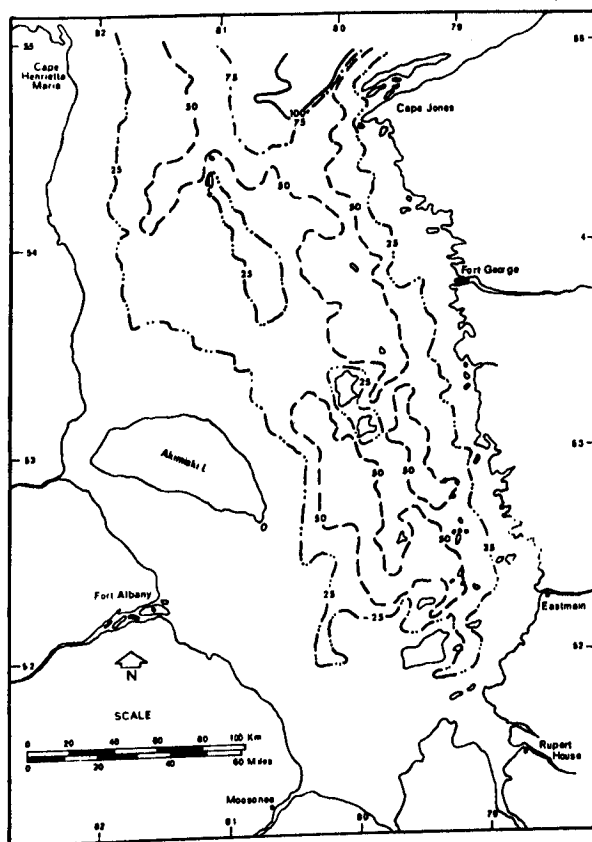


Figure 2: Bathymetry of James Bay

The deepest part of James Bay is located in the northeast corner and reaches a maximum depth of a little over 100 metres. The rest of James Bay is extremely shallow with only a small portion reaching depths larger than 50 metres. The bathymetric data collected during

the 1975 and 1976 winter surveys was used to obtain a new bathymetric map of James Bay using 25-metre depth contours (Figure 2). Bathymetric data was available on a 6.25-kilometre grid throughout James Bay with the exception of the permanent open-water area below Akimiski Island. Even with this amount of data it is still hard to determine if the sill north of Akimiski Island extends completely across the bay. The deep-water exchange with the southern part of the bay thus might be restricted by this sill to a depth of 50 metres. To the south of the sill, some parts of the bay have depths of 65 metres, although most of the area is less than 25 metres deep. In general, the western side of the bay is very shallow and has a gentle topography, while the eastern side is deeper with a more rugged topography. The bay has an average depth of 28.5 metres, an average width of 150 kilometres, and a length of about 400 kilometres. In comparison to Hudson Bay, this represents 1/11th of the surface area of Hudson Bay and 1/70th of its volume.

2.2 Oceanographic Parameter Distributions of Hudson Bay

The oceanographic circulation in Hudson Bay will be a major factor in determining the oceanographic parameter distribution and circulation of James Bay. Only summer oceanographic "station" data is available in Hudson Bay for determination of the general circulation patterns. All available data up to 1962 was presented by Barber (1967) for Hudson Bay and again in 1972 with particular emphasis on James Bay. New oceanographic "station" data for Hudson Bay was collected during the multi-disciplinary survey on board the vessel CCGS Narwhal by Ocean and Aquatic Sciences, Central Region, of the Department of Environment (Baird, 1975). The data was collected underway by means of a CSTD probe inside a "fish" whose surface values were calibrated against independent values of surface water samples. Some 300 station locations were sampled (Prinsenbergh, 1977a) of which 222 were used to obtain the surface salinity and temperature distribution of Figures 3 and 4 respectively. The 222 stations were occupied between August 12 and September 29 with most of them occurring in the northern half of the bay during the latter part of August and in the southern half of the bay during the last three weeks of September. Both figures reveal an anti-clockwise surface drift associated with the Coriolis effect

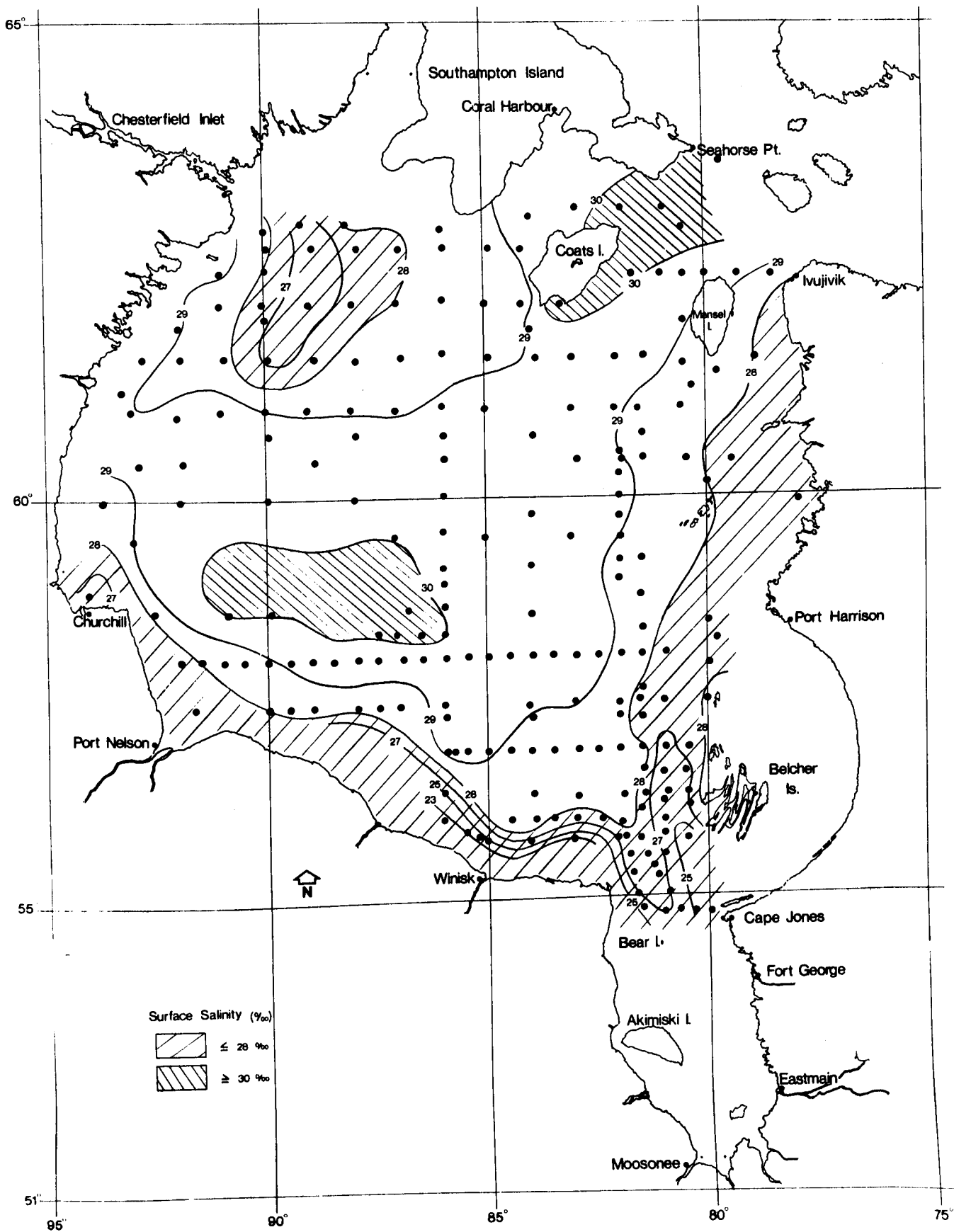


Figure 3: Surface Salinity Distribution of Hudson Bay for the Summer of 1975

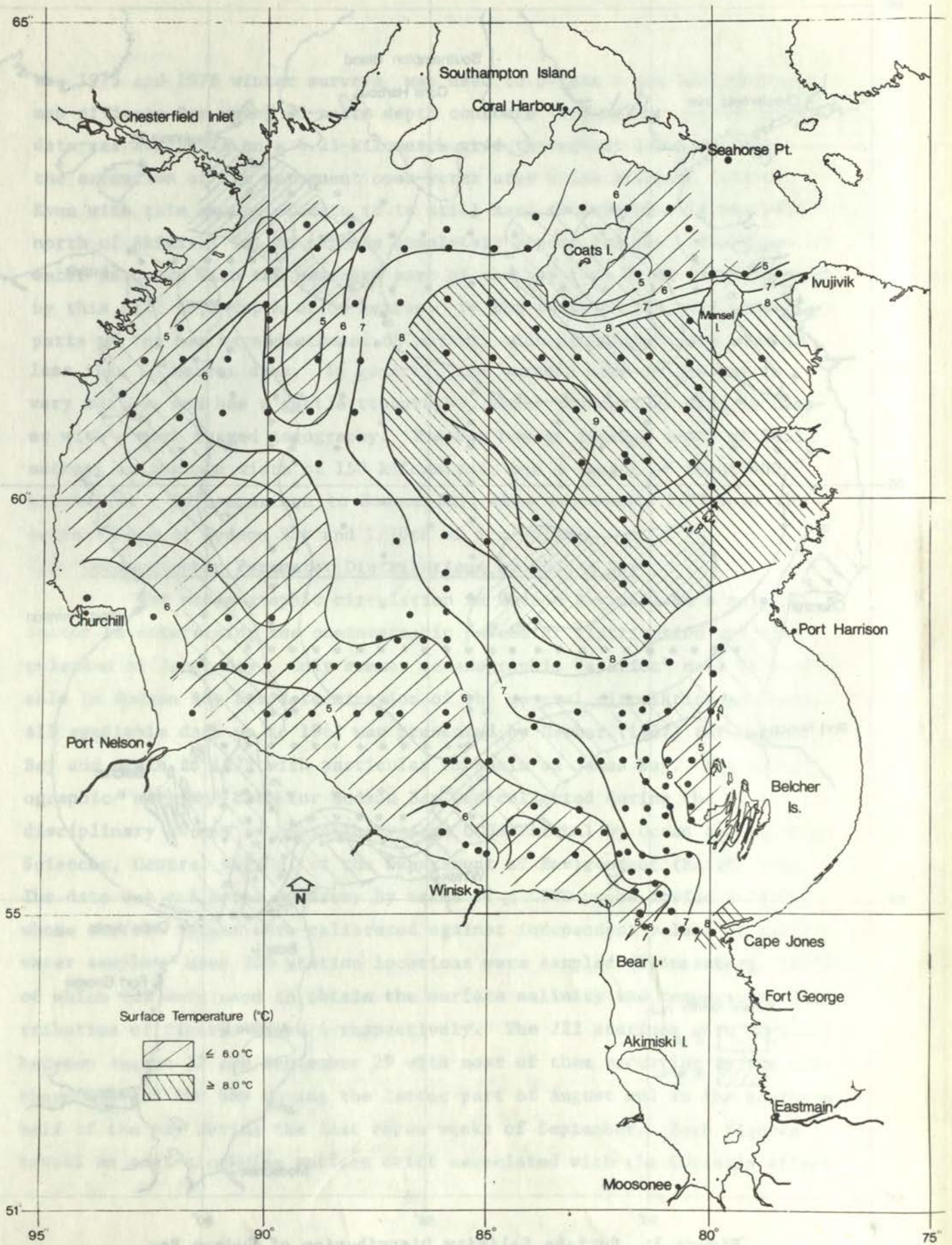


Figure 4: Surface Temperature Distribution of Hudson Bay for the Summer of 1975

in semi-enclosed basins of the northern hemisphere. Murty and Yuen (1973) showed theoretically that this occurs in Hudson Bay. The figures show that there is a westerly drift of cold and high salinity water entering from Hudson Strait through the two northerly channels. A south to south-westerly drift of cold and low salinity water can be traced from Chesterfield Inlet, and a southeasterly drift of cold and low salinity water can be associated with the outflows of the southern major rivers (Nelson and Churchill). A cell of warm and low salinity water can be followed out of James Bay in a northerly direction. The warm surface water in the center and northeasterly area of the bay shows that this water has been exposed to surface heating longer than the remaining water, which is in agreement with the generally earlier ice breakup in the southeast and eastern area as well as with the anti-clockwise surface drift.

Surface and sub-surface waters are mixed when tidal or wind-induced currents encounter an area with a shallow and rugged topography. The resulting increase in turbulent mixing decreases the surface temperature and increases the surface salinity value by bringing up some colder and more saline sub-surface water into the surface layer. The resulting surface-mixed water will then drift away with the general current and can be used as an indicator of the surface current's direction. The shallow, rugged topography in the vicinity of the Belcher Islands induces this type of turbulent mixing. The cold and high salinity surface water (Figures 3 and 4) to the northwest of the islands indicates a northerly surface drift west of the islands.

Surface drift currents can be obtained using an approximate form of the total three-dimensional conservation of salt equation:

$$\frac{\partial S}{\partial t} + U \frac{\partial S}{\partial x} + V \frac{\partial S}{\partial y} + W \frac{\partial S}{\partial z} = \frac{\partial}{\partial x} K_x \frac{\partial S}{\partial x} + \frac{\partial}{\partial y} K_y \frac{\partial S}{\partial y} + \frac{\partial}{\partial z} K_z \frac{\partial S}{\partial z} \quad (2.1)$$

where $\frac{\partial S}{\partial t}$ is the local rate of change in S, salinity; U, V, and W are the mean velocities; and K_x , K_y , and K_z are the eddy coefficients of diffusion in the x, y, and z directions, respectively. When a steady-state condition and only horizontal processes are assumed to occur in the surface

layer, equation (2.1) reduces to:

$$U \frac{\partial S}{\partial x} + V \frac{\partial S}{\partial y} = K_x \frac{\partial^2 S}{\partial x^2} + K_y \frac{\partial^2 S}{\partial y^2} \quad (2.2)$$

Equation (2.2) can be used to obtain velocity distribution for areas where horizontal salinity tongues are present. The tidal currents u and v for Hudson Bay, as found by Freeman and Murty (1976), were used to obtain the coefficients of diffusion similarly to the Irish Sea study by Hunter (1975). The tidal currents and diffusion coefficients are related by the equations:

$$K_x = (c_1 u^2 + c_2 v^2) / [u^2 + v^2]^{\frac{1}{2}} \quad (2.3)$$

$$K_y = (c_1 v^2 + c_2 u^2) / [u^2 + v^2]^{\frac{1}{2}} \quad (2.4)$$

where $c_1 = 65,000$ cgs and $c_2 = 3,300$ cgs. An advection current along the central axis of the Chesterfield Inlet plume of 4.0 cm sec^{-1} can be obtained from equation (2.2) and the salinity distribution of Figure 3. Similarly, the advective currents in and out of James Bay to the west of the Belcher Islands are 4.5 cm sec^{-1} and 2.0 cm sec^{-1} , respectively. The range of eddy coefficients along the major tidal axis used to obtain these currents was from 1.3×10^6 to 4.9×10^6 cgs, but, since only the tidal portion of the total currents was used, these coefficients and the derived currents are minimum values. The surface drift current amplitude of the anti-clockwise circulation of Hudson Bay is thus expected to be at least 5.0 cm sec^{-1} .

The current of the Chesterfield Inlet tongue can be determined in another independent way by considering the time required to move the head of the tongue from the mouth of the inlet at the start of freshet on June 18th to the position in which it was observed on August 15th some 345 kilometres from the mouth of the inlet. Over the total time span of 61 days, the front of the tongue moves at an average speed of 6.5 cm sec^{-1} as compared to 4.0 cm sec^{-1} obtained by the advection/diffusion method, using the salinity distribution observed during the last two weeks of August. In order to check whether the fresh water of the salinity tongue

is actually supplied by the Chesterfield River system, a freshwater volume of $3.0 \times 10^3 \text{ m}^3$ was calculated relative to a base salinity of 28.5 ‰ . The total outflow volume from May 1 to August 15 for Chesterfield Inlet came to $2.6 \times 10^3 \text{ m}^3$ (Prinsenber, 1977b) and compares favourably with the above volume calculated from the oceanographic "station" data.

2.3 Oceanographic Parameter Distributions of James Bay

Summer oceanographic observations in James Bay have been hampered by the large number of shallow and uncharted areas and by weather conditions. Large vessels are able to withstand the numerous northwesterly storms characteristic of the area but have not surveyed much of the shallow, uncharted areas of the southern and eastern parts of the bay. Smaller vessels have been used to carry out oceanographic surveys of the shallow areas of the La Grande and Eastmain estuaries; but data collection is then very weather-dependent, and large time gaps between sets of data exist. Therefore, most of the summer data available for James Bay is for the northern half of the bay with some coverage of the southern half obtained during the winter surveys of 1975 and 1976.

Surface salinity and temperature data in the northern part of James Bay, collected during September of 1972 (Pullen, 1973), are shown in Figure 5. The surface distribution features observed in Hudson Bay (Figures 3 and 4) during the summer of 1975 continue into James Bay. The cold and relative high-salinity water of Hudson Bay enters in the western half of James Bay, and a narrower tongue of warm and low-salinity water leaves James Bay in the eastern half. Hudson Bay figures (3 and 4) represent data collected in late August of 1975, while the James Bay data was collected in the middle of September, 1972. If year-to-year variations were negligible, the difference in the 1972 and 1975 distributions would indicate the extent of surface cooling and river dilution experienced in the fall. However, the yearly winter weather and ice patterns have a major affect on the summer oceanographic distributions in the Hudson/James Bay region, and a large variability in regional distribution exists. Larnder (1968) states, with regard to the ice cover of Hudson Bay, that "the pattern of formation and break-up differs widely from year to year and from one locality to another." This can be seen in the yearly ice data of

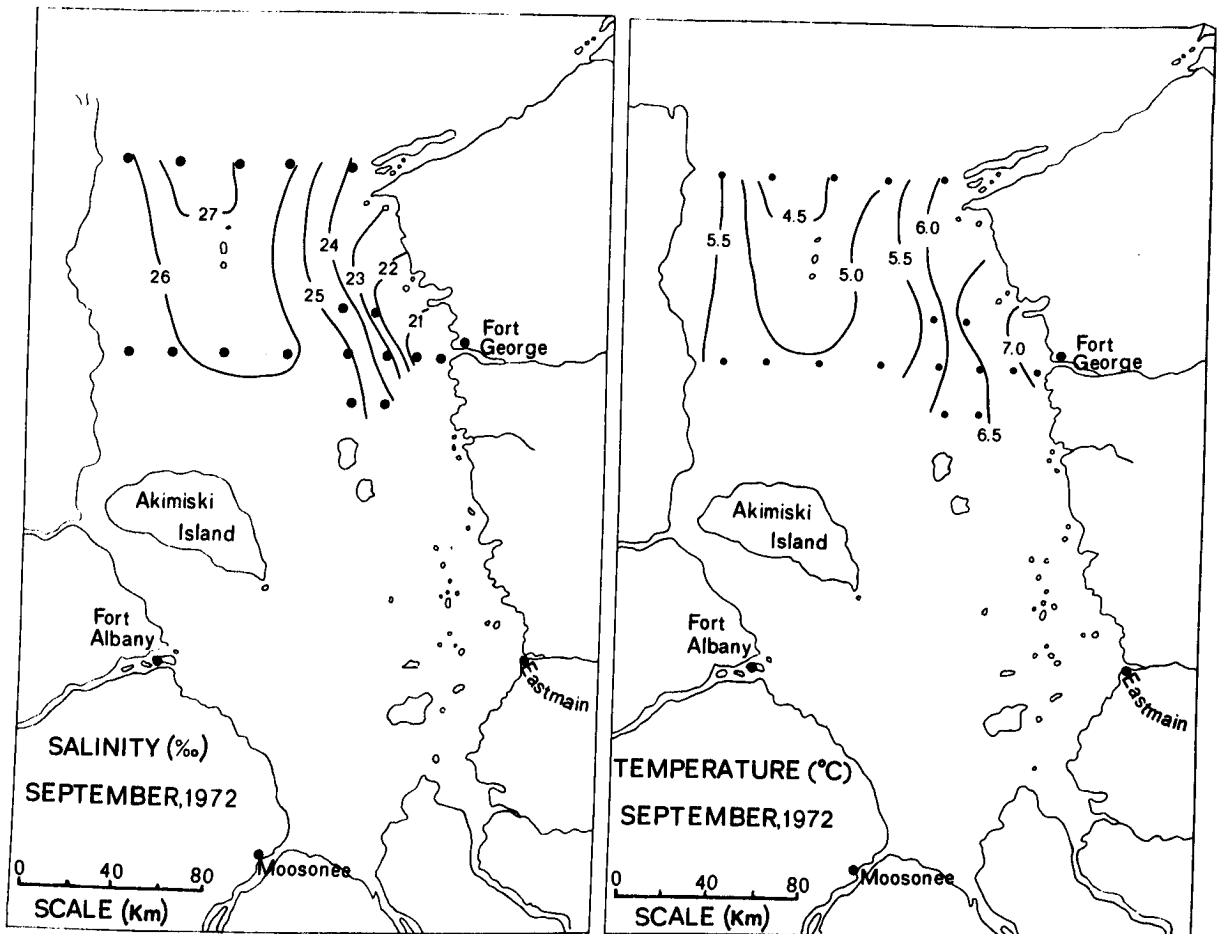


Figure 5: Surface Salinity and Temperature Distribution of James Bay for September 1972

"Hudson Bay and Approaches" (Environment Canada). The variability of the yearly ice pattern will thus be reflected in the variability of the summer oceanographic distributions. The surface distribution alone cannot be used for the simple advection-diffusion approximation which was used to obtain surface drift currents in Hudson Bay. The source of the fresh water is now too close to the observation area, and a vertical estuarine circulation thus determines the salinity distribution of James Bay.

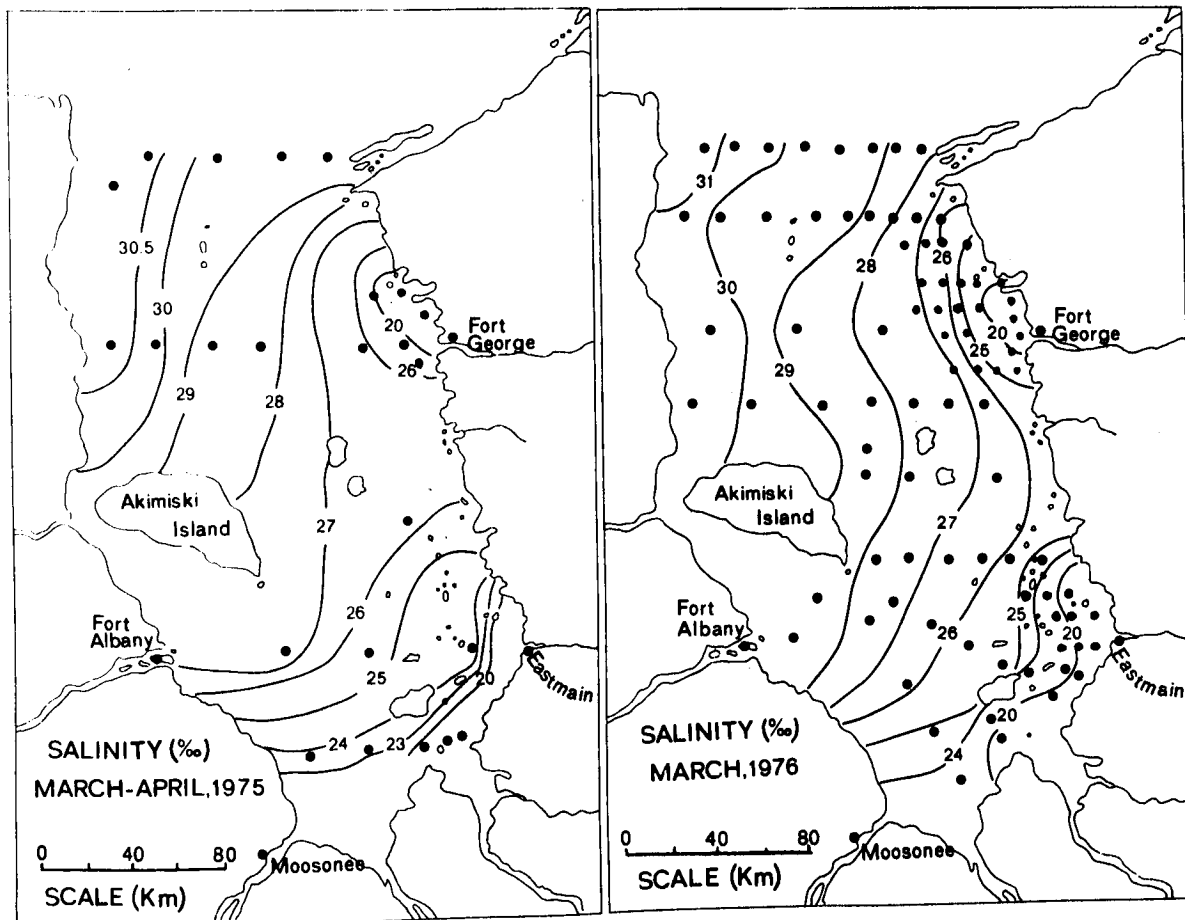


Figure 6: Surface Salinity Distributions of James Bay for the Winters of 1975 and 1976

The horizontal salinity distribution at 2-metres depth for the 1975 and 1976 winters are shown in Figure 6 (Peck, 1976b). Water of high salinity ($30 - 31 \text{ ‰}$) enters James Bay along the west coast and is diluted by the freshwater input from the rivers as it drifts cyclonically in James Bay. The Coriolis force deflects the diluted water to the right and restricts the outflow of the less saline water ($28 - 29 \text{ ‰}$) into a surface boundary current along the east coast. Compared to the summer salinity distribution, the winter salinity values are high. The large change in the pycnocline present in the summer months has not been re-established after the vertical overturning of the water column at the time of ice formation. March and April are the two months when a maximum

ice cover is present. Vertical stability is re-established when fresh water is added to the top of the water column by both river discharge and ice melt.

The vertical salinity, temperature, and density structure at the entrance area of James Bay is shown in an east-west cross-section diagram of Figure 7 and a north-south cross-section diagram of Figure 8. The east-west cross-section consists of the "1975 CCGS Narwhal" stations 17 to 21 and is taken as the boundary between Hudson Bay and James Bay and is called transect 1. The depth profile of the east-west sections shows the deep-water region at the eastern side of the bay (stations 19, 20, and 21), but, as shown in Figure 1, this region does not extend too far into the bay itself. The warm and low salinity water (less dense) is deflected by the Coriolis force to the eastern side as it leaves the

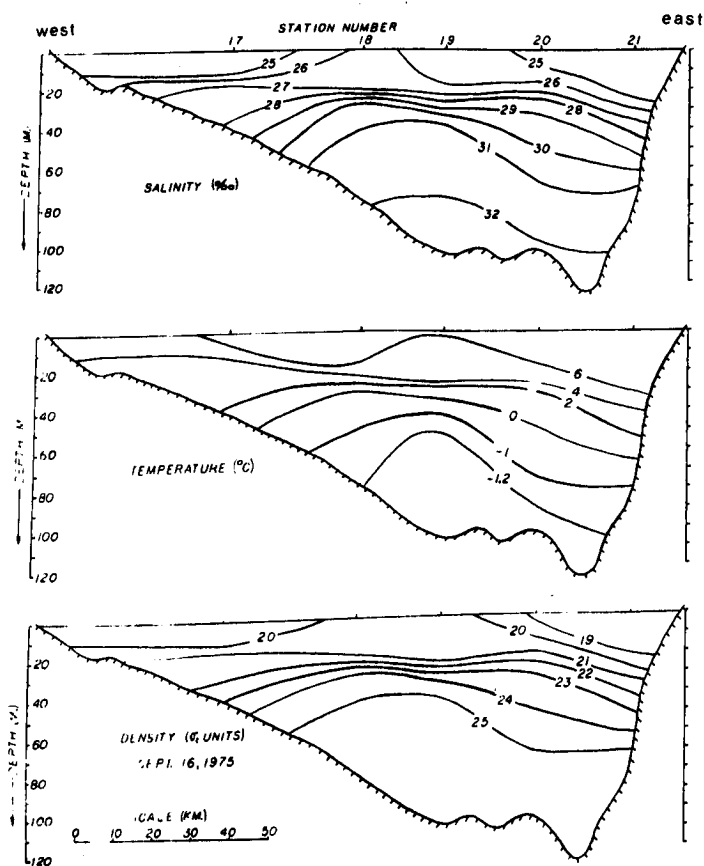


Figure 7: Cross-Sectional (West-East) Salinity, Temperature, and Density Distributions at the Entrance of James Bay

bay. The inflowing water of Hudson Bay also has a low salinity portion to the right of the flow direction but is not as warm. Both water masses are well separated from the deeper water by a sharp pycnocline. The western part of the pycnocline is not as well defined due to a higher degree of turbulent tidal mixing over the shallow topography. The pressure gradient caused by the internal density structure will add to the pressure gradient term of the surface slope (freshwater cells on both coasts) so as to decrease the currents with depth. On the eastern side, the sum of the pressure gradients actually reverses sign with depth and results in a small inflow over the entire deeper layer.

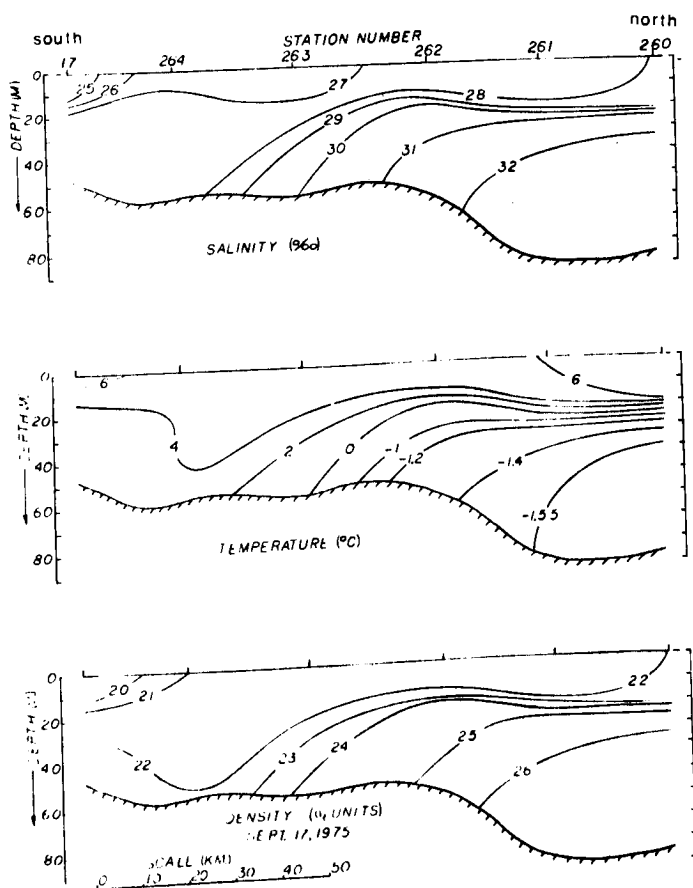


Figure 8: Cross-Sectional (South-North) Salinity, Temperature, and Density Distributions North of the Entrance of James Bay

The north-south cross-section starts at station 17 (entrance of James Bay) and runs due north to station 260, where the sill separating the deep waters of James Bay and Hudson Bay is located. The bottom layer cross-sectional features are similar to estuarine patterns as cold saline water is slowly eroded by vertical diffusion as it moves along the bottom into James Bay. The features of the surface layer are more difficult to understand without the knowledge of the general circulation pattern of the Hudson Bay waters of the area. The surface water of the cross-section increases in salinity and decreases in temperature as the inflowing Hudson Bay water is crossed diagonally between stations 17 and 260. The sharp pycnocline extends over all the Hudson/James Bay region and was found between depths of 15 to 30 metres, depending on weather conditions and bottom topography.

CHAPTER 3

3.0 Theoretical Determination of the Circulation Contributions

The relative importance of the various contributions to the total circulation of James Bay is investigated by means of the conservation of salt equation, an estuary classification method using stratification and circulation parameters, and an estuarine circulation model. The upstream salt flux at the entrance of the bay is found to be achieved mainly by advection so that, when a steady-state approximation can be used, simple Knudsen's relationships can be used to obtain the in- and outflow current values from the river runoff rate and salinity data. The analytical model is used to provide velocity and current profiles under various wind conditions.

3.1 Conservation of Salt Equations

In order to understand the circulation and oceanography of James Bay completely, it would be necessary to solve seven equations relating seven variables: salinity, temperature, density, velocities U, V, and W, and surface elevation. The seven equations are the conservation equations of salt, temperature, and mass, the three equations of motion, and the equation of state. These sets of equations can only be handled numerically in approximate forms if a large computer is available or analytically if the system of equations is approximated further to two dimensions. Since salinity is the major variable determining the density in estuarine circulation, the salinity conservation equation is investigated for James Bay to obtain information as to the importance of the various terms. When the three-dimensional conservation equation (2.1) is integrated over the width $b(x)$, the equation reduces to two dimensions with x the longitudinal axis and z the vertical axis of the bay:

$$b \frac{\partial S}{\partial t} + b \left(U \frac{\partial S}{\partial x} + W \frac{\partial S}{\partial z} \right) = \frac{\partial}{\partial x} \left(bK_x \frac{\partial S}{\partial x} \right) + \frac{\partial}{\partial z} \left(bK_z \frac{\partial S}{\partial z} \right) \quad (3.1)$$

where all parameters are now width-averaged quantities. Still no analytical solution is available as long as $\partial S/\partial t$ cannot be ignored relative to the other terms in the equation.

To check the relative amplitudes of $\partial S/\partial t$ for the James Bay area, all available data from two repeated oceanographic station lines between 1972 and 1976 were used. The data was assigned to two volumes, splitting the bay into an upper region of transect areas 1 and 2 (data at latitude $54^{\circ} 46'$) and a lower region of transect areas 3 to 6 (data at latitude $53^{\circ} 50'$); the positions of the areas are shown in Figure 9. A third bottom region of transect area 5 and 6 should actually be used, but not enough data is available from the lower part of James Bay. The data was averaged over the total width for each depth layer and is listed in Tables A-1 and A-2 of the appendix. The resulting data, shown in Figure 10, reveals large data gaps between the summer ice-free period of July 31 to October 14 and the winter period of March 3 to April 1. The gaps become even more significant when the freshwater input (Prinsenber, 1977b) of James Bay is inspected showing that the two observation periods have relative constant input values but are separated by a large input peak during the spring runoff. It is thus impossible to extend the curves outside the actual observation periods, and the winter and summer data can only be treated separately. Throughout the summer, the bottom salinity at the entrance of the bay (transect 1) decreases slightly, while the surface salinity increases significantly. The sectional mean salinity value of transect 1 decreases, since all the layers below 25 metres experience a decrease in the salinity value as the summer progresses. During this time, the freshwater input of James Bay is going through its summer minimum value between the fall and spring peak runoffs. There seems to be a time lag between the occurrence of the spring freshwater input taking place primarily in the southern part of the bay and the occurrence of the surface minimum salinity value of transect 1 in the northern part of the bay. For a time lag of two months and a separation distance of 290 kilometres, a minimum surface drift of 5.6 cm sec^{-1} can be obtained for the freshwater effect to move up along the coast of Quebec.

The amplitude of the local rate of change of salinity for transect 1 can be calculated from the sectional mean salinity values spanning the summer months:

$$\frac{\partial S}{\partial t} = \frac{1 \text{ }^{\circ}/\text{oo}}{75 \text{ days}} = 1.5 \times 10^{-7} \text{ }^{\circ}/\text{oo sec}^{-1} \quad (3.2)$$

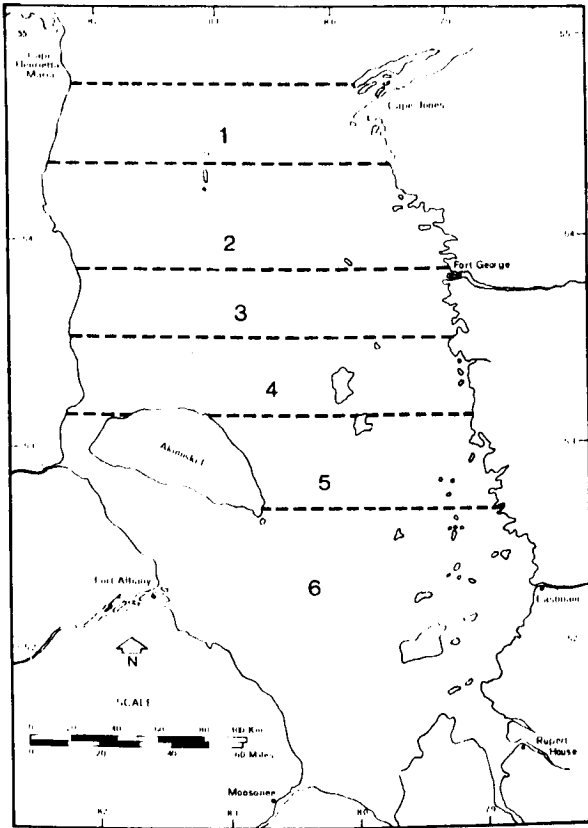
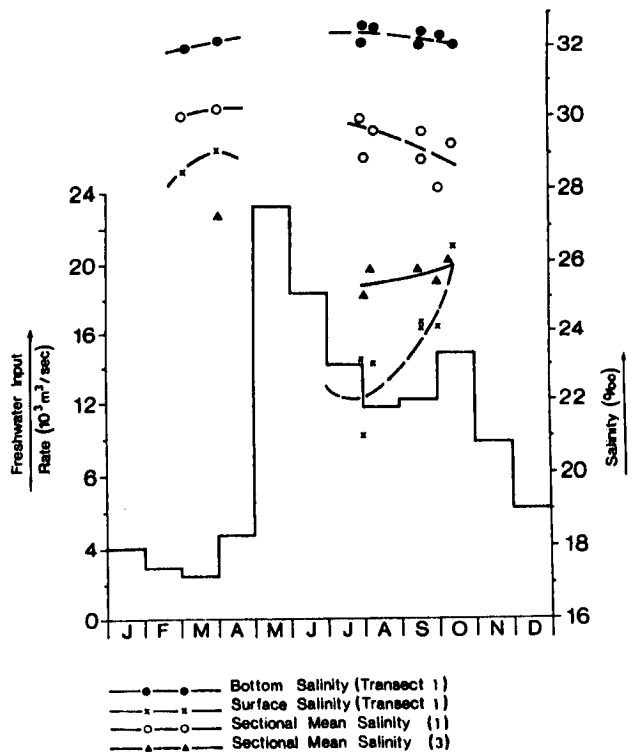


Figure 9: Transect Areas of James Bay used in the Freshwater Input Distribution

James Bay (1972 - 76)

Figure 10: Monthly Freshwater Input and Transect Salinity Values for James Bay



The sectional mean salinity gradient $\partial S/\partial x$ is equal to 3.7×10^{-7} ‰/cm so that, for the local rate of change to be at least an order of magnitude less than the advection $U\partial S/\partial x$, the current (sectional mean) has to be greater than 4.2 cm sec^{-1} . When just the surface layer is considered, a current greater than 11.4 cm sec^{-1} is needed so that the local rate of salinity change is at least an order less than the advection term. Surface currents of this magnitude are observed, but sectional mean currents of 4.2 cm sec^{-1} probably do not occur; which means the local rate of change of salinity cannot be ignored when considering the section as a whole but can be ignored when considering the surface separately.

Figure 10 also shows that the sectional mean of transect 1 decreases in the summer months at a rate of 1.5×10^{-7} ‰ sec^{-1} , while that of transect 3 increases at a rate of $.8 \times 10^{-7}$ ‰ sec^{-1} . When the whole of James Bay is considered and the salinity change of transect 1 represents the northern portion of James Bay ($512 \times 10^9 \text{ m}^3$) and that of transect 3 the southern portion ($1,358 \times 10^9 \text{ m}^3$), the salinity content of the bay is relatively constant. The salinity content only increases at a rate of $.09 \times 10^{-7}$ ‰ sec^{-1} which is 1/20 of the rate at which transect 1 loses salt. This slow increase for the summer months reflects the readjustment of salinity distribution over the entire bay after the large freshwater input during the spring. When the bay is considered as one unit, this small, time-dependent term can be ignored relative to the advection across the mouth, as it will be 40 times smaller for sectional mean currents of 1 cm sec^{-1} in magnitude.

The next relative amplitudes to investigate are the horizontal diffusion and advection for separate layers across the entrance of the bay. The eddy coefficient of diffusion is now simply derived from $K_x = c_1 u$, where, as before, $c_1 = 65,000 \text{ cgs}$ and u is the total tidal velocity which, for a maximum value of 46 cm sec^{-1} , gives an upper limit for the diffusion coefficient of $3 \times 10^6 \text{ cm}^2 \text{ sec}^{-1}$. Using all the available data, a mean surface and bottom (30-40m) salinity gradient was obtained by averaging all summer gradients between transects 1 and 3. From the available current meter data, a surface outward drift of 6.5 cm sec^{-1} and bottom inward drift of 2.7 cm sec^{-1} were used for the width-mean current amplitudes. Using these values and average surface (~5-metre depth) and bottom (35-metre depth) salinity values of 24.5 ‰ and 29.6 ‰, respectively,

the ratio of the horizontal advection to horizontal diffusion was found to be -177 in the surface layer and +111 in the 30- to 40-metre layer. Both show that the diffusion is two orders of magnitude less than the advection. The change in sign reflects the fact that while diffusion of salt is always into the bay, advection is out of the bay in the surface layer and into the bay in the lower layer.

When the salt exchange across the entrance is further approximated to advection in a two-layered system, the salt influx is overestimated since the salt diffusion into the bay is ignored. In the resulting equations, the current into the bay of the lower layer is larger than it will be if diffusion is retained. The conservation of salt and mass equations are now reduced to Knudsen's relations:

$$A_1 U_1 S_1 = A_0 U_0 S_0 \quad (3.3)$$

$$A_1 U_1 + R = A_0 U_0 \quad (3.4)$$

where A is the cross-sectional area of each layer, R the freshwater input, and the subscripts "i" and "o" refer respectively to the inflow of the bottom layer and the outflow of the surface layer. The layers were considered to be separated at a mean depth of 14 metres. For a summer freshwater input rate of $11.8 \times 10^3 \text{ m}^3 \text{ sec}^{-1}$, a surface layer salinity of 26.0 ‰ and area of $21.3 \times 10^5 \text{ m}^2$, and a bottom layer salinity of 30.9 ‰ and area of $81.1 \times 10^5 \text{ m}^2$, the equations will result in a bottom layer inflow of .78 cm sec^{-1} and a surface layer outflow of 3.52 cm sec^{-1} , which are approximately 1/3 the mean values calculated from current meter data. The discrepancy is due partly to the omission of diffusion and partly to the bay's readjustment to the much higher freshwater input of the spring (twice as large as the summer mean).

3.2 Analytical Models

Analytical circulation models can provide valuable information on the relative importance of the driving mechanism in estuarine problems. Although existing models can handle only two-dimensional, steady-state circulation and are restricted in resolving bottom topographic features,

they have been used very successfully in predicting the salinity and current distribution of narrow estuaries. James Bay is not actually a narrow estuary but, since the only available models use this approximation, it will be assumed here so that the wind-driven and freshwater contributions to the circulation can be investigated without going into numerical techniques.

Similarity solutions for the estuarine circulation have been developed in several papers by Hansen and Rattray (1965, 1966, 1967), and their results will be applied to James Bay. Their solutions and classifications for the estuary depend upon a stratification and a circulation parameter determined from observable boundary conditions, while a third independent parameter can also be used when the wind stress is important.

The stratification parameter is the ratio of the top to bottom salinity difference ΔS to the mean salinity value of the vertical cross-section S_0 . The circulation parameter is the ratio of the net surface current U_s to the mean freshwater current U_f through the vertical cross-section; the latter is obtained by dividing the total rate of freshwater discharge R_0 passing through the cross-section with the cross-sectional area A . The stratification and circulation parameters are used in the estuarine classification to obtain the relative diffusive fraction of the total upstream salt flux under zero wind stress conditions. The analytical solutions provide a means to determine the relative importance of the circulation contributions due to freshwater discharge, horizontal density gradient, and wind stress. Solutions, however, are only possible when the longitudinal variation of the eddy coefficients is appropriate in relation to that of the width, depth, and river discharge, any of which may vary as a power or an exponential function of the longitudinal coordinate. The eddy coefficient values are determined by the tidal currents and cannot include any dependence on the vertical structure of the salinity distribution of the mean circulation. Away from the river mouths, both the horizontal salinity gradient and the top-to-bottom salinity difference of many estuaries are nearly constant over a considerable distance. For these conditions, solutions are possible if the vertical viscosity and diffusivity coefficients are constant and the horizontal diffusivity coefficient has a seaward gradient equal to the mean freshwater

velocity through the section. Closer to the river mouths, the vertical salinity difference is not constant but is more nearly proportional to the mean salinity over any section. Solutions are then possible if both diffusivity coefficients are constant and the vertical viscosity coefficient varies exponentially in the longitudinal axis. The solutions for the first type of estuary will be used for James Bay, while the second type are more applicable for the La Grande River estuary.

The density ρ used in the equations of motion is assumed to be dependent only on salinity S by:

$$\rho = \rho_0 (1 + \epsilon S/S_0) \quad (3.5)$$

where ρ_0 is the density of fresh water and ϵ is the constant changing the salinity parameter into density units. The equations of motion used are:

$$\frac{\partial P}{\partial x} = \frac{\partial}{\partial z} (\rho N_z \frac{\partial U}{\partial z}) \quad (3.6)$$

and
$$\frac{\partial P}{\partial z} = \rho g \quad (3.7)$$

where ρ is the pressure and g the gravitational acceleration. The eddy viscosity N_z , like the eddy diffusivity, is assumed independent of the vertical structure of the mean flow and salinity distribution. Eliminating the pressure between (3.6) and (3.7) and using the Boussinesq approximation yields a vorticity equation of the mean flow:

$$\frac{\partial^2}{\partial z^2} (N_z \frac{\partial U}{\partial z}) = \frac{g}{\rho} \frac{\partial \rho}{\partial x} \quad (3.8)$$

The equation of continuity is used to write the velocities in the form of a transport streamfunction ψ :

$$\frac{\partial \psi}{\partial z} = -bU \text{ and } \frac{\partial \psi}{\partial x} = bW \quad (3.9)$$

where b is the average width of the bay.

When the salinity is non-dimensionalized by $\theta = S/S_0$, then the equation of the conservation of salt and equation (3.8) can be written in terms of ψ and θ :

$$\frac{\partial \psi}{\partial x} \frac{\partial \theta}{\partial z} - \frac{\partial \psi}{\partial z} \frac{\partial \theta}{\partial x} = + \frac{\partial}{\partial x} (bK_x \frac{\partial \theta}{\partial x}) + \frac{\partial}{\partial z} (bK_z \frac{\partial \theta}{\partial z}) \quad (3.10)$$

$$\frac{\partial^2}{\partial z^2} [N_z \frac{\partial}{\partial z} (\frac{1}{b} \frac{\partial \psi}{\partial z})] + \epsilon g \frac{\partial \theta}{\partial x} = 0 \quad (3.11)$$

The above two equations, subject to the appropriate boundary conditions, are the governing equations for the circulation and salinity distribution in the estuary. Further simplicity can be achieved by non-dimensionalizing the vertical and horizontal coordinates by:

$$R = z/H \quad \text{and} \quad \bar{x} = \frac{1}{S_0} \frac{\partial S_0}{\partial x} x \quad (3.12)$$

where H is the mean depth of the estuary and $\partial S_0/\partial x$ is the horizontal gradient of the cross-sectional mean salinity. Another way to write the horizontal coordinate is by the usage of the constant v which represents the diffuse fraction of the total upstream salt flux and relates diffusive upstream salt flux at $x = 0$, $K_x \partial S_0/\partial x$, and the total salt flux given by the product of the sectional mean velocity and the sectional mean salinity:

$$K_x \frac{\partial S_0}{\partial x} = vU_f S_0 \quad (3.13)$$

The horizontal coordinate can thus also be represented by:

$$\bar{x} = vU_f K_x x \quad (3.14)$$

when the sectional mean salinity gradient is not available.

The similarity solutions to equations (3.10) and (3.11) are:

$$U = U_f \left[\frac{3}{2} (1-\eta^2) + \frac{T}{4} (1-4\eta+3\eta^2) + \frac{vRa}{48} (1-9\eta^2+8\eta^3) \right] \quad (3.15)$$

$$\text{and } S = S_0 (1 + \bar{x}) + \frac{S_0}{M} \left[f_1(\eta) + \frac{T}{4} f_2(\eta) + \frac{\nu Ra}{48} f_3(\eta) \right] \quad (3.16)$$

$$\text{where } f_1(\eta) = -37/120 - 1/4\eta^2 - 1/8\eta^4, \quad (3.17)$$

$$f_2(\eta) = -1/20 + \eta^2/2 - 2\eta^3/3 + \eta^4/4, \quad \text{and} \quad (3.18)$$

$$f_3(\eta) = -1/12 + \eta^2/2 - 3\eta^4/4 + 2\eta^5/5. \quad (3.19)$$

The constants in equations (3.15) and (3.16) are the dimensionless wind stress T , the estuarine Rayleigh number Ra , and the tidal mixing parameter M and are given by:

$$T = H\tau(N_z U_f \rho_0)^{-1} \quad (3.20)$$

$$Ra = \epsilon g H^3 (N_z K_x)^{-1} \quad (3.21)$$

$$M = S_0 K_z (\partial S_0 / \partial x U_f H^2)^{-1} \quad (3.22)$$

where τ is the surface wind stress. The theoretical solution, equations (3.15) and (3.16), is comprised of three independent contributions: 1) freshwater contribution; 2) wind-driven contribution; and 3) the gravitational contribution to the circulation. They can thus be used to investigate the relative importance of the three contributions as well as the fractional composition of the inward salt flux by diffusion and advection.

As can be seen from equations (3.13) to (3.22), a large number of parameters are required before a velocity and corresponding salinity distribution can be calculated. Some of the parameters, such as ν , equation (3.13), are obtained from the sectional mean salinity gradient which may be obtained from the available data. Other values for the parameters, such as the eddy coefficients K_z , K_x , and N_z used for determining the values of the parameters T , Ra , and M , are sometimes difficult to establish since the eddy coefficients are dependent upon the magnitudes of the tidal and wind-induced currents and the stability of the density structure. Some of these values needed in equations (3.15) and (3.16) can also be derived by means of bulk parameters. Bulk parameters are dependent upon three quantities, each having the dimensions of velocity:

the freshwater discharge per unit cross-sectional area U_f ; the RMS tidal current speed U_t ; and an internal speed value U_d derived from the density difference $\Delta\rho$ between the river and sea water. The internal speed value is defined by:

$$U_d = \sqrt{gH\Delta\rho/\rho} \quad (3.23)$$

For well-mixed and partially-mixed estuaries, a densimetric Froude number defined as $F_m = U_f/U_d$ expresses the ratio of forced river flow to the potential density-induced internal flow. Theoretical studies of Ippen (1966) have shown the importance of the densimetric Froude number in the dynamics of stratified estuaries. It correlates with the estuarine Rayleigh number used here, which expresses a similar ratio of flows. Hansen and Rattray (1966) showed that the two are approximately related to each other by:

$$\nu Ra = 16 F_m^{-3/4} \quad (3.24)$$

The other bulk parameter couples the circulation and salinity distribution and is defined by the ratio $P_m = U_f/U_t$. It expresses the tidal mixing as was similarly done by the parameter M and was shown by Hansen and Rattray (1966) to be related to it by:

$$M/\nu = .05 P_m^{-7/5} \quad (3.25)$$

The ratio parameters P_m and F_m could thus be used to replace the eddy coefficients or used as another independent check on the values of M/ν and νRa needed to obtain the velocity and salinity distributions.

The bulk parameter ratio F_m can also be used to independently check the value of the circulation parameter U_s/U_f . This can be done by evaluating equation (3.15) at the surface ($\eta=0$) so that it reduces to:

$$U_s/U_f = 3/2 + T/4 + \nu Ra/48 \quad (3.26)$$

where νRa is obtained from equation (3.24). Classification of an estuary by means of the stratification and circulation parameters can thus be achieved without the knowledge of the surface currents.

3.3 Estuarine Classification

Parameters defined in the above analytical model can also be used to classify the estuary by means of the stratification and circulation properties. For several seasonal periods where salinity distributions were available, the circulation parameter U_g/U_f was obtained from the bulk parameters using equation (3.26) for the zero wind stress condition. Only the circulation parameter value for the summer months of August and September could be checked by the available surface current meter data. The surface current value obtained from equation (3.26) was found to be 11.4 cm sec^{-1} and compared very well with those mean drift values measured over the same time period at 10-metre depths. Mean drift values of 16.4 cm sec^{-1} and -3.3 cm sec^{-1} were found on the Quebec side and at the middle of the James Bay entrance, respectively. These values, when averaged and extrapolated towards the surface, would give a surface mean drift of around 8 cm sec^{-1} . The bulk parameter equation (3.26) seems to provide adequate mean surface current values and was used for the summer months as well as the other seasons for which salinity data was available.

Figure 11 shows the classification diagram on which values for transect 1 (entrance of James Bay) and transect 3 (Fort George) were plotted. The actual values of the stratification and circulation parameters are listed in Table A-3 of the appendix. The comparative importance of horizontal diffusion and advection for the upstream salt flux is represented by the diffusive fraction constant ν . The value of the constant varies between 0 and 1. A value of $\nu=1$ means that the gravitational convection ceases and upstream salt flux is entirely by diffusion, whereas, as ν approaches a zero value, the diffusion is unimportant and the upstream salt flux is almost entirely by gravitational convection in a two-layered flow. The total classification region of Figure 11 can be split into four areas depending on the value ranges of $\Delta S/S_0$, U_g/U_f , and ν . When U_g/U_f is less than 2.0, the net flow is seaward at all depths, and the upstream salt transfer is effected by diffusion. For values of $\Delta S/S_0$ less than 1.0 and ν between

.01 and 1.0, the net flow reverses at depth, and both advection and diffusion contribute to the upstream salt flux. For values of ν less than .01, the upstream salt flux is by advection, as is the case for the two James Bay transects in the summer. Fjord estuaries are usually considered to fall into this classification area when $\Delta S/S_0$ is greater than .1 as well. The lower layer is so deep that, in effect, the salinity gradient and the circulation do not extend to the bottom. The last classification area is the salt wedge found in the top left-hand corner with high stratification and low circulation parameter values. The Strait of Juan de Fuca (between Vancouver Island and Olympic Peninsula) was plotted as a comparison and is also a fjord but with a slightly smaller stratification parameter.

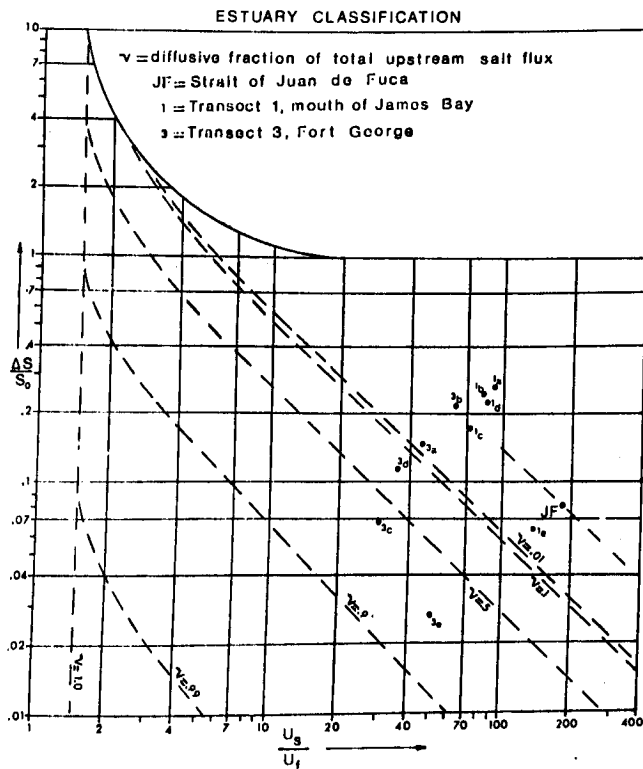


Figure 11: Estuary Classification of James Bay Transects 1 and 3

The derived parameters for the James Bay entrance, transect 1, all fall above the $v=.01$ line. This means that all the upstream salt flux at the entrance is accomplished by advection, which is characteristic for a fjordal-type circulation. Three salinity distributions during the summer months of August and September are represented by: l_a , when an average depth of 74.4 metres is taken for the transect 1 area; l_b , when an average depth of 54.2 metres is used for the combined area of transects 1, 2, & 3; and l_c , during the fall when the two available salinity distributions reveal that the entrance area becomes less stratified but still behaves as a stratified fjord. When all five sets of salinity distributions are used, average open-water parameters are obtained and represented by l_d . Under ice-covered conditions, the entrance area l_e still behaves as a fjord but under less stratified salinity conditions.

The subscripts of the points representing transect 3 represent the same salinity data set as those subscripts of transect 1. The average depth of transect 3 is only 33.9 metres, restricting the bottom flow. The difference in the circulation for the less shallow transect 3 is that, during the fall (3_c) and winter (3_d), both diffusion and advection become important in the upstream salt flux. Even for the mean open-water condition (3_d) when the five summer salinity distributions are used, the upstream salt flux of the transect 3 region is accomplished to some extent by diffusion. The characteristics of the fjordal estuarine circulation as found at the entrance of the bay thus changed to that of a partially-mixed estuary of transect 3. The classification diagram therefore agrees with the findings of section 3.1 in that, when considering James Bay as one region, the advective terms dominate the diffusive terms in the upstream salt flux, and Knudsen's relation can be used when a steady-state condition can be assumed. Within James Bay, both terms are important. The diffusion of salt upstream within James Bay buffers the estuary against salinity changes induced by changes in the freshwater input. If the freshwater input was to increase, the horizontal gradients and thus the upstream salt diffusion increase to offset the dilution caused by the larger freshwater input.

CHAPTER 4

4.0 Analytical Results

The analytical estuarine model is applied to James Bay for both the ice-free summer season and the ice-covered winter season. For the summer, results are presented for zero wind condition and for small southerly and large northerly wind conditions. The ice cover of James Bay, although not landlocked, is very restricted in its movement and currents beneath it will experience a surface boundary which retards the surface flow. Instead of forcing an exact zero flow condition at the ice-water interface, a small surface current is kept as the ice is not completely landlocked. Circulation due to wind is not considered during the winter season of James Bay; the ice cover inhibits the wind effect from the water. For an ice cover which is free to move and which has intense ice ridging, the wind stress is transmitted to the water as the ice pack moves with the wind due to ice form and skin drag (Arya, 1975). The effect of friction exerted by the ice on the moving water beneath it is treated as a negative wind stress. Winter results are shown for the present runoff rate and for the predicted runoff rate upon completion of the hydroelectric development on the La Grande River.

4.1 Summer Analytical Results

The theoretical streamfunction solution, equation (3.15), can be split into three contributions whose comparative magnitudes depend upon the dimensionless wind stress T , the estuarine Rayleigh number Ra , and the diffusive fraction constant ν . The three contributions to the circulation are: the freshwater contribution, required for disposal of the input of freshwater; the gravitational contribution, due to the density difference between fresh and salt water; and the wind-driven contribution, mostly confined to the surface. Their velocity profiles are normalized by the surface velocity of the freshwater contribution whose $[1 - (z/H)^2]$ depth-dependence produces only a seaward flow at all depths. When the wind stress is zero, the gravitational contribution can cause a reversal of velocity with depth producing an inward bottom flow. The gravitational

contribution depth-dependence is $[1 - 9(z/H)^2 + 8(z/H)^3]$, and its amplitude is dependent on the estuarine analog of the Rayleigh number. Under zero wind stress conditions, the freshwater and gravitational contributions will produce a vertical velocity distribution which has a surface layer outflow and a bottom layer inflow. The amplitudes of the flow are related to each other since the total volume transport is related to the freshwater input when the salt transport is conserved. The amplitude and direction of the wind-driven contribution are dependent upon wind stress τ . For a positive wind stress (southerly wind for James Bay), the wind-driven contribution will cause a surface outflow and a bottom return flow. Its depth-dependence is $[1 - 4(z/H) + 3(z/H)^2]$ and conserves volume transport for each transect but depends on and combines with the other two contributions in the conservation of salt transport through each transect. For a northerly wind, the surface wind drift can reverse the direction of the combined surface outflow of the freshwater discharge and gravitational contributions leading to a three-layer flow distribution with an inflow on the surface and bottom and an outflow just below the shallow wind-induced surface flow.

The analytical model was applied to James Bay for both summer and winter conditions. During the summer, some current meter data was available in addition to the required salinity distribution. The salinity and velocity profiles for the entrance transect 1 and the Fort George transect 3 are shown for the summer condition in Figure 12. Each individual diagram shows the theoretical profiles for three different wind conditions: zero wind; a small southerly wind ($T/4=28$); and a larger northerly wind ($T/4=-120$). A $T/4=28$ value represents a wind stress caused by a 5.0-knot southerly wind, while a $T/4=-120$ value represents a wind stress of a 15.0-knot northerly wind. Meteorological summer data from Moosonee and Great Whale weather stations (published monthly by Environment Canada), as well as the data collected by the survey vessels and the 1975 meteorological buoy at the entrance of James Bay, all show that the mean wind direction in the summer is from the west and southwest with an average strength of 10 knots, while winds during storms can reach up to 30 knots

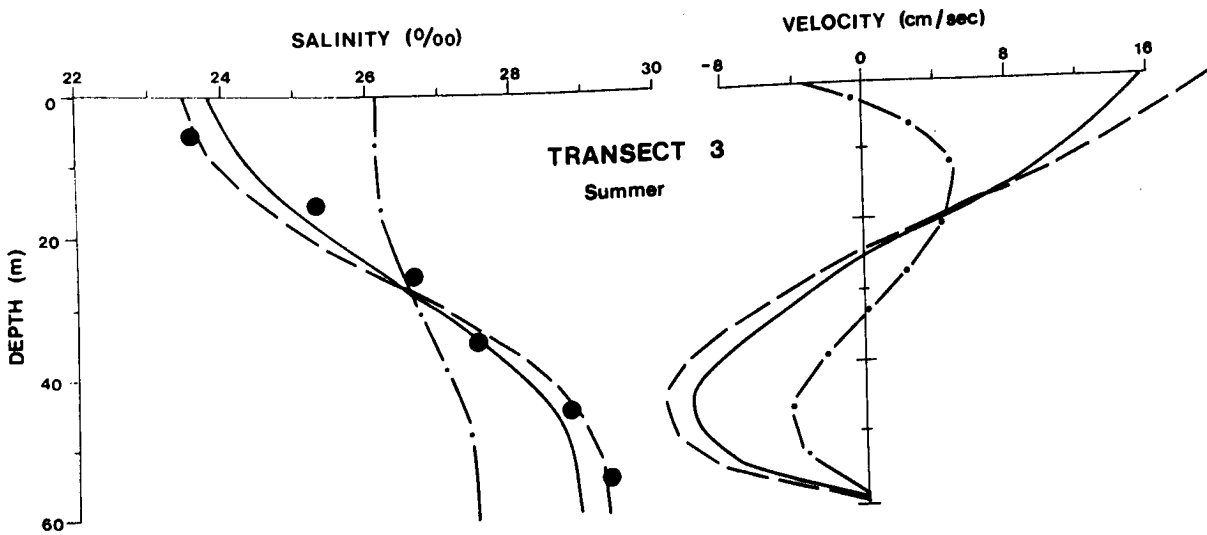
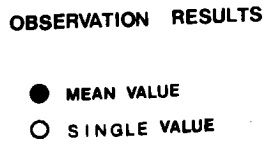
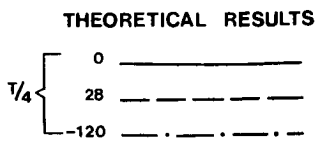
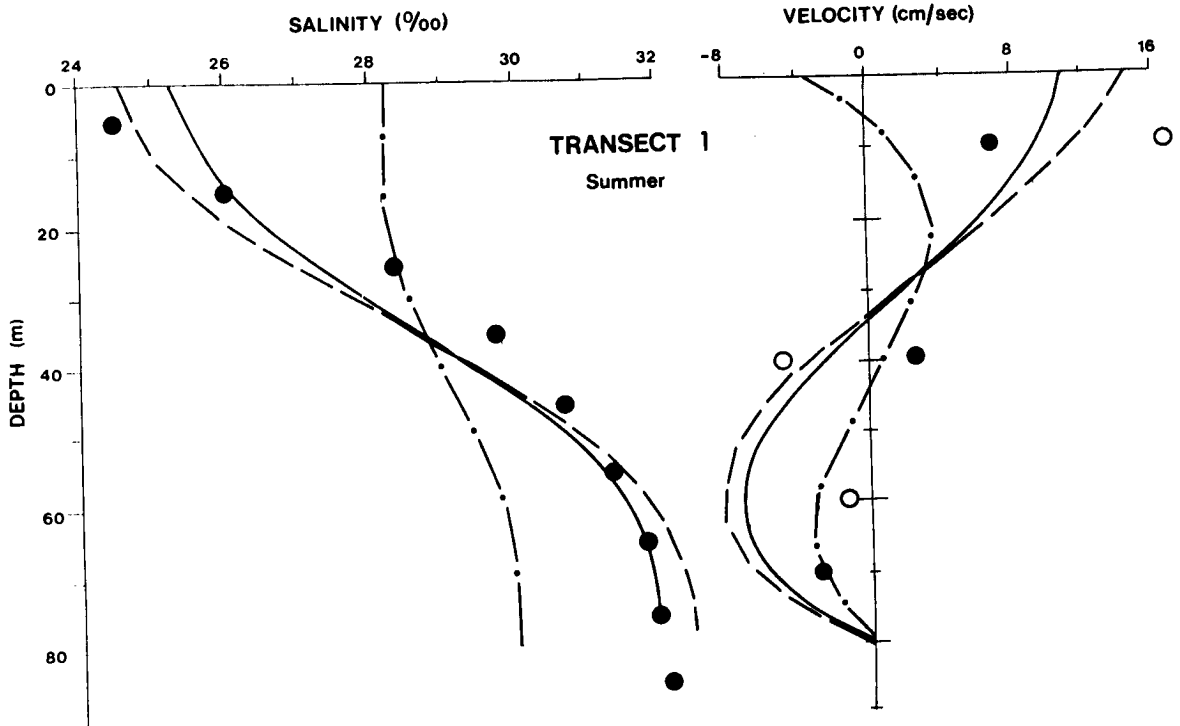


Figure 12: Analytical and Observational Results for different Summer Wind Stress ($T/4$) Conditions (Positive velocity value means a flow out of the bay, northward)

and be from any direction. The observed surface data shown in Figure 12 also suggest that the analytical salinity results agree best with the salinity data when a small southerly wind component is used in the model. The salinity data plotted was calculated from three data sets taken during the 1972 and 1973 surveys which cover both areas of transects 1 and 3. The data for August and September were used since the current meters deployed during the summer of 1975 collected data only during these two months. The observed salinity data agrees well with that predicted by the model. The only deviation between the predicted and observed salinity profiles is that the model cannot predict the sharp halocline because it uses a constant vertical eddy coefficient and not one that is dependent on the vertical density and horizontal velocity shear.

The corresponding velocity profiles for the same three wind conditions are also shown in Figure 12. Equation (3.15) shows that the velocity values are normalized by the mean drift velocity U_f caused by the total freshwater contribution passing through each transect. The monthly values of mean drift velocities were calculated from the total freshwater input that enters upstream from the transect. The freshwater input results from river discharge and the net precipitation and evaporation. The monthly freshwater totals for each transect section are listed in Table A-4 and were taken from the "Freshwater Budget of Hudson Bay" (Prinsenber, 1977b). The corresponding monthly mean drift velocities were calculated from these by dividing the input rates by the cross-sectional area for each transect. The results are listed in Table A-5 of the appendix. For the same observation period (1 August to 18 September), the mean drift velocity for transects 1 and 3 was $11.4 \times 10^{-2} \text{ cm sec}^{-1}$ and $15.7 \times 10^{-2} \text{ cm sec}^{-1}$, respectively. These values are two orders of magnitude smaller than the actual surface velocity values predicted by the model or observed by the current meters. Thus, the volumetric addition effect of freshwater on the current directly is not the main cause for the circulation. The freshwater dilution effect on the density structure causes a horizontal pressure gradient which is the main contributor to the circulation in the form of gravitational circulation.

The model velocity profiles of transects 1 and 3 show that a small southerly wind (5.0 knots) increases the velocity of the surface outflow and, due to conservation of salinity, will also increase the velocity of the bottom inflow. For a larger northerly wind (15.0 knots), the surface outflow current is reversed so that a small surface layer inflow is present. The corresponding maximum velocity value of the bottom inflow layer is reduced and the outflow layer is now present just below the immediate surface in order to conserve the total salinity transport through each transect. Under these conditions, the vertical salinity profile at each transect becomes nearly homogeneous, although the mean horizontal salinity gradient is still present. The observed velocities plotted in Figure 12 consist of mean values for which two available values at the same depth were averaged as well as some single values which are either the only available data at that depth (i.e. 60 metres) or extreme values. Figure 13 shows the locations of the current meters whose long-term mean current values were used in Figure 12. The actual observed mean values are listed in Table A-6 of the appendix.

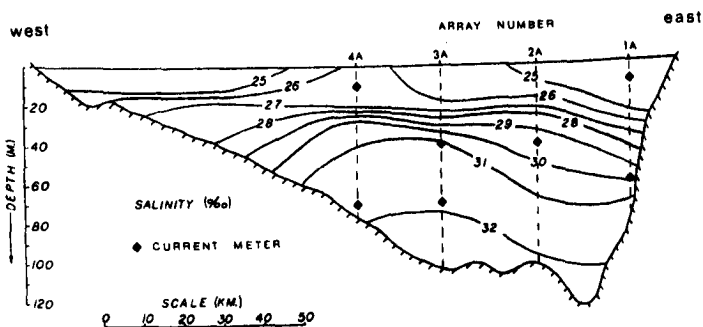


Figure 13: Locations of Current Meters Relative to Salinity Distribution as observed during Retrieval of Meters (September 17, 1975)

The three mean values are at 10-, 40-, and 70-metre depths. They underestimate the theoretical results for both the surface outflow and bottom inflow values and on first inspection may correlate better with theoretical results for a small northerly wind condition. However, when looking at the extreme values plotted at depths of 10 metres (Array #1A) and 40 metres (Array #3A), the theoretical results for a small southerly wind condition underestimated the observed values. The assumed cross-sectional homogeneity required for the analytical solution is actually not found in a wide estuary such as James Bay. The Coriolis effect (discussed in 4.2) deflects the surface outflow water to the right, so that most of the outflow is actually present only in the eastern half of the entrance. The surface current meter at the middle of the entrance (Array #4A), which is used to obtain an average surface outflow at the 10-metre depth, is located at a salinity value that is found at the 33-metre depth at Array #1A for September 16, 1975 (Figure 13). When it is referred to the mean salinity profile used in the model run for the summer condition, the surface current meter in the middle of the estuary would have to be relocated to a depth of 19 metres. Similarly, the surface meter of Array #1A would be relocated to a depth of 3 metres. This would be a useful way to relocate all the current meter depths and obtain a better correlation with the theoretical model prediction if concurrent salinity data covering the region of transects 1 and 3 and current meter data were available. The current meter data was collected during the summer of 1975 while a salinity distribution covering the top half of James Bay is available for the summers of 1972 and 1973. Thus, not enough data is available to relocate the current meter depths according to the in-situ mean salinity value and a mean reliable salinity profile covering the total time period of observation.

The observed mean current values underestimate the predicted model values, while extreme single values overestimate them. The predicted current profiles for transect 3 are shown in Figure 12 for the same three wind conditions. For a small southerly wind, the surface current reaches a speed of 19 cm sec^{-1} with a maximum inflow current of 11

cm sec⁻¹ at a depth of 44 metres. No observed current meter data is available for comparison, although the corresponding salinity profile of the model agrees well with the observed salinity data.

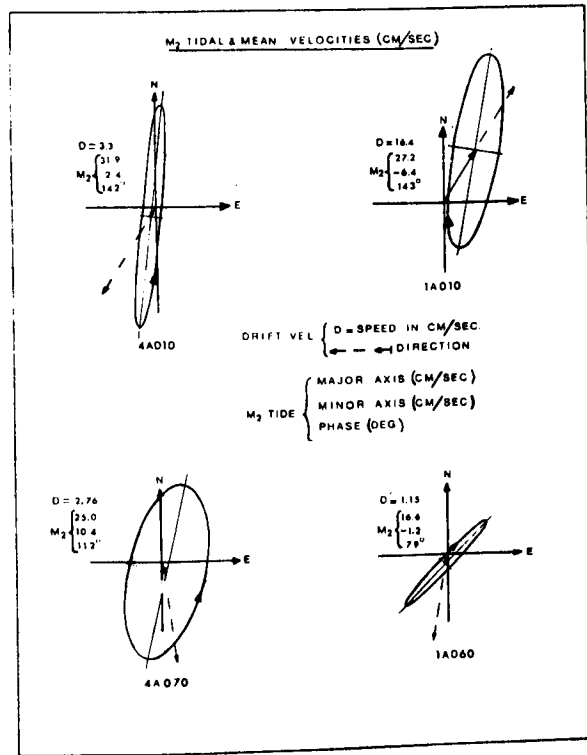


Figure 14: Tidal (M₂) and Mean Velocities for Four Current Meters located at 10-Metre Depth at Arrays 1A and 4A, 60-Metre Depth at Array 1A and 70-Metre Depth at Array 4A

The tidal (M_2) and mean current velocities for data from four of the current meters are shown in Figure 14. Array #1A is located off the Quebec coast, while Array #4A is located in the middle of the entrance of James Bay (see Figure 13). The surface meter of Array #1A is located in the surface outflow, while all the other current meter data show an inflow. The surface outflow has a speed of 16.4 cm sec^{-1} and is directed toward the region between the Belcher Islands and the Quebec mainland. A small inward flow of 1.15 cm sec^{-1} is present at the 60-metre depth. The M_2 tidal current has an amplitude of 27.2 cm sec^{-1} at the surface and 16.6 cm sec^{-1} at the 60-metre depth. The latter shows the interaction with the bottom features and has a reduced amplitude relative to the surface tidal current. The results of the array in the middle of the entrance (#4A) show a small inward mean velocity at the two depths with some change in direction, showing alignment with the bottom topography. The M_2 tidal currents are, at each corresponding depth, larger than those of Array #1A and, as well, have an opposite sense of rotation. Both results were predicted by the numerical solution of the tides in Hudson Bay (Freeman and Murty, 1976).

4.2 Coriolis Effect

The analytical model of the estuarine circulation has ignored the Coriolis effect, causing the isopycnals to dip down toward the eastern shore. The relative change of the observed velocities with depth can be checked against the cross-sectional slope of the isopycnals by the relation:

$$\frac{\partial \rho}{\partial y} = \frac{f}{g} \frac{\partial(\rho U)}{\partial z} \quad (4.1)$$

where ρ is the density, f the Coriolis parameter, and g the constant of gravity. When the density is rewritten in sigma-t notation and values of f and g for the entrance of James Bay are used, the relation can be further reduced to:

$$\frac{\partial \sigma_t}{\partial y(\text{km})} = .121 \frac{\partial U(\text{cm sec}^{-1})}{\partial z(\text{m})} \quad (4.2)$$

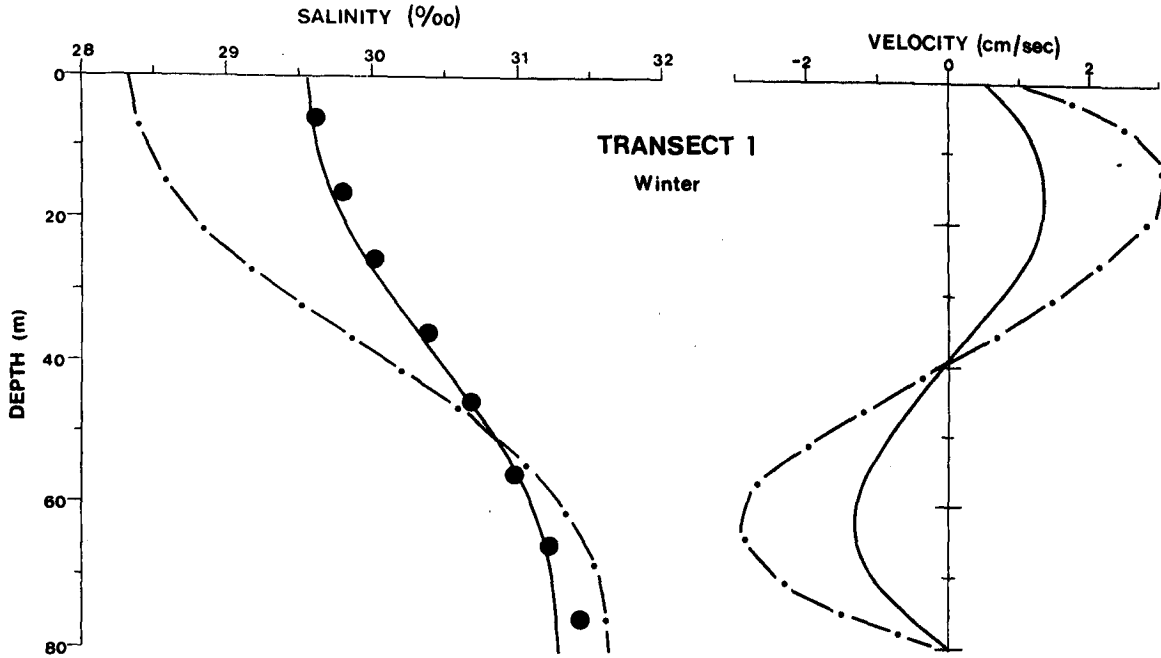
Between Arrays #1A and #2A, the density structure changes about 1.8 σ_t units over their separation distance of 26.5 kilometres in the first 40 metres and on the average of 1.0 σ_t units between 40- and 60-metre depths. The total change in drift current U between the 10- and 60-metre depths will be 23.07 cm sec⁻¹ for the density structure at September 16. This is made up of a velocity change of 16.83 cm sec⁻¹ between the 10- and 40-metre depths and 6.24 cm sec⁻¹ between the 40- and 60-metre depths. Since stratification slowly increases during the summer, this value was larger than the 14.96 cm sec⁻¹ value found for the density structure at the time of deployment of instruments on July 31. An average value of the two is 19.02 cm sec⁻¹ which is close to the change in the observed drift velocities of 17.55 cm sec⁻¹ between the 10- and 60-metre depth of Array #1A. Knudsen's relation gave only a 4.3 cm sec⁻¹ change for the in- and outflowing currents. However, this value was obtained from cross-sectional mean currents rather than from a specific station profile, such as station #1A where the largest velocity change with depth was observed. Also, Knudsen's relation gives only mean velocity values for each layer rather than specific values at a particular depth.

The summer model results for zero wind stress will have a mean surface layer velocity value of 8 cm sec⁻¹ when the surface layer is considered to extend to 33 metres. An average velocity value for the remaining bottom layer is 4 cm sec⁻¹. The model predicts a velocity change between the inflow at the bottom and the outflow at the surface of 12 cm sec⁻¹ in comparison to the value of 4.3 cm sec⁻¹ found by Knudsen's relation. The change of velocity with depth calculated from the isopycnal slopes thus compares directly with the observed current meter data when extreme values are taken. When cross-sectional values, or layer mean values, are used from either observed velocity data or model results, the velocity change with depth is underestimated in comparison to the value found from the density structure. It is even more underestimated by the results obtained when using Knudsen's relation. However, these and the cross-sectional mean values do not take into account the Coriolis effect which intensifies the surface outflow on the Quebec shore.

Velocity changes with depth can thus be inferred from observed mean density distributions when enough density data is available to average out the density variation caused by tidal currents. To obtain absolute velocity values, the assumption of steady-state conditions for salt and volume has to be used. The relative velocity profiles between the stations are re-adjusted until conservation of salinity for the total transect is satisfied. This method was applied to the James Bay summer data by El-Sabh and Koutitonsky (1977) and produced geostrophic current values for October comparable to the observed summer current meter data.

4.3 Winter Analytical Results

During the winter months, ice cover inhibits the transfer of wind stress to the water. The friction of the landlocked ice pack on the currents moving beneath it can be regarded as a negative wind stress which acts in the opposite direction from the outflowing surface layer. The observed winter salinity distribution of 1975 was used to obtain the horizontal sectional mean salinity gradient $\partial S_0 / \partial x$, the product of the diffusive fraction constant, and the estuarine Rayleigh number νRa , from equation (3.24) in a similar manner to that done for the summer data. The present winter conditions have only a small freshwater mean drift velocity value U_f of 2.35×10^{-2} cm sec⁻¹. This is 1/4 of the value of U_f used for the summer condition, as can be seen from Table A-5 of the appendix. The model salinity and velocity results and the observed salinity data are shown in Figure 15. The model was run with a negative surface stress value which produced nearly zero surface current. A small surface current was kept, as the ice in James Bay can move in response to currents. Both salinity profiles of the analytical model correlate very well with the observed mean profile values. The pycnocline is not as sharply defined as during the summer so that a constant vertical eddy coefficient, which represents the same degree of vertical mixing for the total water column, is a good approximation. The predicted winter current values are very much smaller than those observed and predicted for the summer conditions under normal wind stress cases. The surface in-

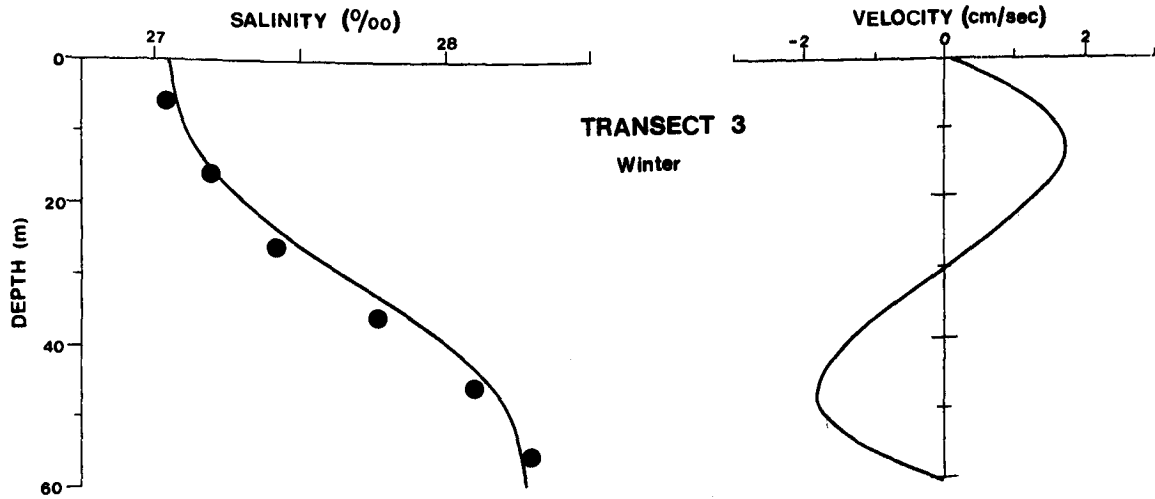


THEORETICAL RESULTS

U_t

 $\left\{ \begin{array}{l} 2.35 \times 10^2 \text{ cm/sec} \text{ ——— PRESENT} \\ 5.25 \times 10^2 \text{ cm/sec} \text{ - · - · FUTURE} \end{array} \right.$

● PRESENTLY OBSERVED VALUES



————— **PRESENT and FUTURE RESULTS**

Figure 15: Analytical and Observational Results for the Present and Future Predicted Winter Conditions (Positive velocity means a flow out of the bay, northward)

and outflow currents for the entrance of James Bay have a maximum speed of only 1.4 cm sec^{-1} as compared to 7 and 11 cm sec^{-1} , respectively, for the summer in- and outflow. At transect 3, the maximum currents for the in- and outflows are 1.7 cm sec^{-1} . No current observation data is available to compare with these analytical results.

4.4 Possible Salinity and Current Changes Due to the La Grande River Hydroelectric Development

The hydroelectric development of the La Grande River will alter the river's seasonal runoff rates to a constant rate of $3.4 \times 10^3 \text{ m}^3 \text{ sec}^{-1}$. The yearly mean runoff rate will double with the additional water coming from the Eastmain River and the headwaters of the Koksoak River presently draining into Ungava Bay. James Bay's yearly mean freshwater runoff will increase by 6.5% at the expense of Ungava Bay, but of more importance are the temporal and spatial changes that will be caused in the monthly runoff rates. During the summer, the total freshwater runoff into James Bay will be reduced by only 5% so that no noticeable change is expected for the total James Bay region. Only local changes will be present in the immediate region around the La Grande/Eastmain River deltas. During the ice-covered season of January to April, the average runoff rate of the La Grande River will increase by 470% above its present rate of $.52 \times 10^3 \text{ m}^3 \text{ sec}^{-1}$. The total runoff rate into James Bay will increase from 3.45×10^3 to $6.06 \times 10^3 \text{ m}^3 \text{ sec}^{-1}$, a gain of 75%. When the evaporation and precipitation rates are included (Prinsenberg 1977b), the mean freshwater drift velocity U_f for transect 1 will increase for the month of March from its present value of $2.35 \times 10^{-2} \text{ cm sec}^{-1}$ to $5.25 \times 10^{-2} \text{ cm sec}^{-1}$.

In order to predict the expected changes in the current and salinity distributions by the analytical model, the upstream conditions of transect 3 were kept the same as before. Although changes are expected here due to the reduction in the winter runoff rate of the Eastmain, the reduction of the current by this drop in runoff rate at transect 3 will be offset by an increase in current upstream as a result of the increased runoff rate of the La Grande River. The other input variable for the

analytical model is the mean salinity gradient which was estimated from the present winter and summer values and assumed to be linearly related to their corresponding mean drift velocity values. Results of the expected future current and salinity distribution are shown in Figure 15.

The cross-sectional mean current speeds more than double from their maximum in- and outflow values of 1.4 cm sec^{-1} to 3.2 cm sec^{-1} , respectively. The mean salinity structure becomes more stratified as the surface salinity value reduces by $1.25 \text{ }^{\circ}/\text{oo}$ and the bottom value increases by $.3 \text{ }^{\circ}/\text{oo}$. The increase in current reduces the surface salinity and brings water with a higher salinity further into James Bay. These are cross-sectional mean values and, as seen in the summer data, they underestimate the surface values on the Quebec coast as the Coriolis effect is not taken into account. The outflow current values were twice as large on the Quebec coast as those for the mean values predicted by the model. When the winter outflow current values of transect 1 are also doubled, then, under the present runoff rate condition, the outflow current value will be 2.8 cm sec^{-1} along the Quebec shore and, for the future runoff conditions, 7.5 cm sec^{-1} . At present, a tracer in the surface layer would drift from the La Grande River area to the entrance of James Bay (a distance of 90 kilometres) in 37 days, while after the completion of the hydroelectric development the time would be 14 days. The surface salinity distribution of the mouth of James Bay (Figure 3) suggests that part of the James Bay surface outflow moves directly northward. If this is also true during the ice-covered winter season, then the Belcher Islands (90 kilometres from the entrance of James Bay) could experience some surface salinity dilution caused by the hydroelectric development of the La Grande River. Even at very slow drift velocity values of 2 cm sec^{-1} , the Belcher Islands could be reached in 50 days, while ice-covered winter conditions exist for at least 120 days between January and April.

CHAPTER 5

5.0 Conclusion

This study of the existing oceanographic station and time-series data has reinforced some of the basic assumptions and ideas about the circulation and distribution of oceanographic parameters in James Bay. During the summer months, Hudson Bay waters enter the bay on the western half as well as the total bottom layer with speeds between 1-4 cm sec⁻¹. This water has relatively low salinity values on the surface due to the inflow of large rivers on the southern coast of Hudson Bay but is distinguishable from the remaining surface water on the eastern half of the bay which has even lower salinity values and higher temperature values. The surface outflow at the James Bay entrance is restricted to a depth of 30 metres and reaches speeds up to 20 cm sec⁻¹. The observed density structure agrees with the findings of the vertical velocity distribution of the current meter data.

Analytical investigation of the circulation suggests that for James Bay the circulation is a combination of the wind-driven and gravitational circulations. Wind-driven surface currents become of equal strength to those generated by the gravitational circulation alone for wind speeds of 15 knots. Northerly winds with speeds greater than 15 knots can thus reverse the surface outflow and set up a three-layered velocity profile with inflows at the surface and bottom and an outflow at mid depths. The gravitational circulation is driven by the horizontal density difference between saline water and that which has been diluted through the freshwater input of the rivers. The actual river contribution to the circulation, which disposes the freshwater volume, is negligible on a large scale such as James Bay. Changes in the freshwater budget of James Bay will show up in the gravitational contribution since the horizontal salinity gradient, and thus the density gradient, will be changed. It becomes even more important for the winter circulation of James Bay as this is the only contributor that causes circulation. The friction imposed by the ice on the winter surface outflow currents is included in the circulation as a negative wind stress opposing the

gravitational surface circulation.

The distribution of oceanographic parameters and observed currents places the James Bay entrance area into a stratified fjord classification. This means that during the summer and winter the upstream salt flux at the entrance of the bay is for the most part achieved by advection, with diffusion being negligible. This was also revealed by the inspection of the advection and diffusion terms in the conservation of salt equation. At the transect off Fort George, the circulation properties become more comparable to those of a strongly-stratified, mixed estuary during the summer and a weakly-stratified, mixed estuary during the winter. For both seasons the upstream salt flux is achieved by a combination of advection and diffusion, with diffusion becoming increasingly important as the stratification and current values decrease. During fall and winter, the largest portion of the upstream salt flux is accomplished by horizontal diffusion.

The cross-sectional mean velocity and salinity profiles computed by the analytical model compare well with those obtained from available data. As the model does not take into account the Coriolis parameter, the model predicts only mean values and not the large surface current and low salinity values caused by the intensification of the surface outflow along the Quebec coast. For the winter conditions, model results were obtained for the present runoff condition as well as for the future condition when the hydroelectric development along the La Grande River is completed. Using the same upstream boundary conditions, the future velocity values will more than double. When Coriolis intensification of the surface outflow is also taken into account, a surface dilution of 1 ‰ and the associated increase in stability of the water column could be felt as far as the Belcher Islands after only 50 days from the onset of a permanent ice cover.

REFERENCES

- Arya, S.P.S., 1975. A drag-partition theory for determining the large scale roughness parameter and wind stress on Arctic Pack Ice. AIDJEX Bulletin, No. 28.
- Baird, S.D., 1975. Hudson Bay 1975 Oceanographic Field Report. Field Report Series, Ocean and Aquatic Sciences, Central Region, Environment Canada, Burlington.
- Barber, F.G., 1967. A Contribution to the Oceanography of Hudson Bay. Manuscript Report Series No. 4, Marine Sciences Branch, Department of Mines and Technical Surveys, Ottawa.
- Barber, F.G., 1972. On the Oceanography of James Bay. Manuscript Report Series No. 24, Marine Sciences Branch, Department of Mines and Technical Surveys, Ottawa.
- Canadian Government. Monthly Record, Meteorological Observations in Canada. Atmospheric Environment Service, Environment Canada, Downsview.
- Canadian Government. Ice Summary and Analysis, Hudson Bay and Approaches. Issued annually since 1964. Meteorological Branch, Department of Transport, Toronto.
- Danielson, E.W. Jr., 1969. The Surface Heat Budget of Hudson Bay. Marine Sciences Manuscript Report No. 9, McGill University, Montreal.
- El-Sabh, M.I. and V.G. Koutitonsky, 1977. An Oceanographic Study of James Bay Before the Completion of the La Grande Hydroelectric Complex. Arctic, Volume 30, No. 3.
- Freeman, N.G. and T.S. Murty, 1976. Numerical Modelling of Tides in Hudson Bay. Journal of the Fisheries Research Board of Canada, Volume 33, No. 10.
- Godin, G., 1972. The Tides of James Bay. Manuscript Report Series No. 24, Marine Sciences Branch, Department of Mines and Technical Surveys, Ottawa.
- Hansen, D.V., 1967. Salt Balance and Circulation in Partially Mixed Estuaries. In Estuaries, pp. 45-51. G.H. Lauff, Editor, American Ass. Advance Sci., Washington, D.C. 757 pp.
- Hansen, D.V. and Maurice Rattray, Jr., 1965. Gravitational Circulation in Straits and Estuaries. J. Mar. Res., 23(2): 104-122.
- Hansen, D.V. and Maurice Rattray, Jr., 1966. New Dimensions in Estuary Classification. Limnol. Oceanogr., 11(2): 319-336.

- Hunter, J.R. 1975. The Determination of Current Velocities from Diffusion/Advection Processes in the Irish Sea. Estuarine and Coastal Mar. Sc., 3(1): 43-55.
- Ippen, A.T., 1966, Editor. Estuary and Coastline Hydrodynamics. Engineering Societies Monographs, McGraw-Hill Book Company, Inc.
- Larnder, M.M., 1968. The ice, in Science, History and Hudson Bay, Volume 1. Department of Energy, Mines and Resources, Ottawa.
- McCarthy, J.F. and J.B. Boyd, 1975. James Bay Winter Survey, 1974-75. Final Field Report. The Canadian Hydrographic Service, Ocean and Aquatic Sciences, Central Region, Environment Canada, Burlington.
- Murty, T.S., 1972. Circulation in James Bay. Manuscript Report Series No. 24, Marine Sciences Branch, Department of Mines and Technical Surveys, Ottawa.
- Murty, T.S. and K.B. Yuen, 1973. Balanced Versus Geostrophic Wind-Stress for Hudson Bay. Journal of the Fisheries Research Board of Canada, Volume 30, No. 1.
- Peck, G.S., 1976a. Nearshore Oceanography of James Bay, in James Bay-Environment 1976 Symposium Proceedings, Montréal Société d'Énergie de la Baie James.
- Peck, G.S., 1976b. James Bay Data Report 1973. Ocean and Aquatic Sciences, Central Region, Environment Canada, Burlington.
- Prinsenber, S.J., 1977a. Hudson Bay Oceanography Data Report 1975 Volume 1. Data Report Series No. 77-1, Ocean and Aquatic Sciences, Central Region, Environment Canada, Burlington.
- Prinsenber, S.J., 1977b. Fresh Water Budget of Hudson Bay. Manuscript Report Series No. 5, Ocean and Aquatic Sciences, Central Region Environment Canada, Burlington.
- Pullen, T.W., 1973. James Bay Data Report 1972. Marine Sciences Directorate, Central Region, Department of the Environment, Burlington.
- Wright, B.M., 1976. James Bay Winter Survey 1976. Final Field Report. The Canadian Hydrographic Service, Ocean and Aquatic Sciences, Central Region, Environment Canada, Burlington.

A P P E N D I X

SALINITY (‰) PROFILES OF TRANSECTS 1 AND 3

Transect 1	1972			1973		1975	
	Depth(m)	Aug. 7 - 8	Sept. 18	Oct. 13 - 14	Aug. 1	Oct. 1 - 2	July 31
0 - 10	24.71	26.30	27.19	22.34	25.17	23.69	25.05
10 - 20	26.34	26.73	27.50	25.10	25.23	26.02	25.76
20 - 30	28.68	27.53	27.94	28.85	25.60	28.44	27.41
30 - 40	30.01	29.38	28.53	29.87	27.00	29.85	29.17
40 - 50	30.89	30.69	29.16	30.52	28.42	30.64	30.19
50 - 60	31.54	31.53	30.14	31.13	29.77	31.11	30.79
60 - 70	31.78	31.76	30.68	31.68	30.57	31.49	31.20
70 - 80	32.01	31.97	30.93	31.95	31.13	31.78	31.74
80 - 90	32.07	32.00	31.29	32.40	31.58	32.00	31.80
90 - 100	32.33	32.20	31.69	32.47	32.01	32.05	31.96
100 - 120	32.35	32.32	31.87	32.53	32.14	32.10	32.03
MEAN	29.61	29.55	29.22	28.87	28.03	28.96	28.80

Table A-1. Cross-Sectional Mean Salinity
- Depth Profiles for Transect 1

Transect 3	1972			1973	
	Depth(m)	Aug. 9 - 10	Sept. 14 - 15	Oct. 13	Aug. 1 - 2
0 - 10	24.05	24.85	25.49	21.93	24.59
10 - 20	25.57	25.39	26.07	25.10	25.19
20 - 30	26.73	26.01	26.30	27.14	25.94
30 - 40	27.16	26.91	26.50	28.12	27.03
40 - 50	29.10	28.50	26.90	29.00	27.17
50 - 60	29.40	29.00	26.90	29.70	27.60
MEAN	25.75	25.71	25.99	25.00	25.44

Table A-2. Cross-Sectional Mean Salinity
- Depth Profiles for Transect 3

CIRCULATION (U_g/U_f) and STRATIFICATION ($\Delta S/S_o$)
PARAMETERS OF TRANSECTS 1 AND 3

DATA			CIRCULATION			STRATIFICATION		
Transect #	Obs. Period	# of Obs.	$U_f \times 10^{-2}$ cm sec ⁻¹	U_g cm sec ⁻¹	U_g/U_f	Depth (m)	S_o ‰	$\Delta S/S_o$
1a	Aug. Sept.	3	11.40	10.67	93.6	74.4	29.31	.262
1b	Aug. Sept.	3	11.40	9.30	81.6	54.2	28.45	.245
1c	Oct.	2	12.88	9.35	72.7	74.4	28.44	.171
1d	Aug. Oct.	5	11.99	10.22	85.2	74.4	28.96	.226
1e	April	1	3.36	4.58	136.2	74.4	30.51	.061
3a	Aug. Sept.	3	15.72	6.95	44.2	33.9	25.75	.147
3b	Aug. Sept.	3	15.72	9.45	60.1	54.2	26.87	.214
3c	Oct.	2	17.68	5.27	29.8	33.9	25.68	.067
3d	Aug. Oct.	5	16.50	6.27	38.0	33.9	25.72	.115
3e	April	1	5.40	2.72	50.5	33.9	27.37	.026

Table A-3. Estuarine Classification Parameters for Transects 1 and 3 of James Bay

FRESHWATER INPUT TO JAMES BAY

($10^3 \text{ m}^3 \text{ sec}^{-1}$)

Area Month	1	2	3	4	5	6	Total
Jan.	.034	.796	.027	.038	.048	3.107	4.050
Feb.	-.016	.522	-.012	-.005	.006	2.359	2.854
Mar.	-.003	.427	-.012	-.017	.001	2.015	2.409
Apr.	-.053	.352	-.070	-.050	-.022	4.316	4.473
May	.257	2.497	.242	.139	.155	19.715	23.004
June	.370	3.963	.274	.219	.215	13.764	18.816
July	.336	2.994	.238	.213	.191	9.770	13.745
Aug.	.241	2.266	.200	.169	.162	8.310	11.348
Sept.	.206	2.483	.155	.128	.119	8.067	11.129
Oct.	.297	2.940	.233	.176	.182	10.044	13.872
Nov.	.023	1.915	-.020	-.043	.005	7.192	9.072
Dec.	.018	1.239	.004	.006	.041	4.549	5.857
						mean	10.052

Table A-4. Total Monthly Freshwater Input for Each of the James Bay Areas

FRESHWATER VELOCITY THROUGH EACH TRANSECT

(10^{-2} cm sec $^{-1}$)

Transect Month	1	2	3	4	5	6
Jan.	3.96	5.38	5.64	6.05	7.87	6.75
Feb.	2.79	3.84	4.11	4.47	5.90	5.13
Mar.	2.35	3.23	3.48	3.78	5.02	4.38
Apr.	4.37	6.06	7.31	8.04	10.71	9.38
May	22.47	30.45	35.47	37.90	49.55	42.86
June	18.36	24.60	25.35	26.84	34.86	29.92
July	13.40	17.91	18.19	19.27	24.84	21.24
Aug.	11.08	14.87	15.48	16.37	21.13	18.07
Sept.	10.87	14.66	14.83	15.75	20.41	17.54
Oct.	13.55	18.17	18.63	19.70	25.50	21.83
Nov.	8.86	12.11	12.49	13.55	17.95	15.63
Dec.	5.72	7.82	8.06	8.70	11.45	9.89

Table A-5. Monthly Freshwater Velocity Values through each James Bay Transect

MEAN CURRENTS** FOR JAMES BAY ENTRANCE

Meter #	Depth (m)	Salinity* (‰)	Speed (cm sec ⁻¹)	Direction (degrees)
1A010	10	24.3	16.39	30
1A060	60	29.8	1.15	199
2A040	40	29.4	9.63	11
3A040	40	31.0	4.97	211
3A070	70	31.8	2.74	297
4A010	10	26.7	3.30	212
4A070	70	31.7	2.76	174

* September 16, 1975

** Time period of August 1 to September 15, 1975

Table A-6. Mean Drift Velocity for the Summer of 1975 at the Entrance of James Bay

